

AperTO - Archivio Istituzionale Open Access dell'Università di Torino

**Structural Anatomy of the Ligurian Accretionary Wedge (Monferrato, NW-Italy), and Evolution of Superposed Mélanges**

**This is a pre print version of the following article:**

*Original Citation:*

*Availability:*

This version is available <http://hdl.handle.net/2318/136528> since 2015-12-22T17:37:15Z

*Published version:*

DOI:10.1130/B30847.1

*Terms of use:*

Open Access

Anyone can freely access the full text of works made available as "Open Access". Works made available under a Creative Commons license can be used according to the terms and conditions of said license. Use of all other works requires consent of the right holder (author or publisher) if not exempted from copyright protection by the applicable law.

(Article begins on next page)



# UNIVERSITA' DEGLI STUDI DI TORINO

**This is an author version of the contribution published on:**

Questa è la versione dell'autore dell'opera:

*Festa et al. (2013) -Geological Society of America Bulletin, v.9 (1), 1580-1598*

doi: 10.1130/B30847.1

The definitive version is available at:

La versione definitiva è disponibile alla URL:

<http://gsabulletin.gsapubs.org/>

**Structural Anatomy of the Ligurian Accretionary Wedge (Monferrato, NW-Italy),  
and Evolution of Superposed Mélanges**

<sup>1</sup> Andrea Festa, <sup>2-1 & 3</sup> Yildirim Dilek, <sup>4-1</sup> Giulia Codegone, <sup>1</sup> Simona Cavagna, and <sup>5</sup> Gian Andrea Pini

<sup>1</sup>Dipartimento di Scienze della Terra, Università degli Studi di Torino, 10125 Torino, Italy

<sup>2</sup>Department of Geology and Environmental Earth Science, Miami University, Oxford, OH 45056, USA

<sup>3</sup>State Key Laboratory of Geological Processes and Mineral Resources, School of Earth Science & Mineral Resources, China University of Geosciences, Beijing 100083, China

<sup>4</sup>Dipartimento di Ingegneria dell'Ambiente, del Territorio e delle Infrastrutture, Politecnico di Torino, 10129 Torino, Italy

<sup>5</sup>Dipartimento di Scienze Biologiche, Geologiche e Ambientali, Università di Bologna, 40127 Bologna, Italy

**Corresponding Author:**

Andrea Festa

Email: [andrea.festa@unito.it](mailto:andrea.festa@unito.it)

**Re-Submitted to:**

Geological Society of America Bulletin

*Revised: 20 April 2013*

## Abstract

We document in this study the internal structure of the Late Cretaceous–late Oligocene Ligurian accretionary wedge in northwestern Italy, and the occurrence in this exhumed wedge of broken formation and three different types of mélanges that formed sequentially through time. The *Broken Formation* is the oldest unit in the accretionary wedge and shows bedding-parallel boudinage structures, which developed as a result of layer-parallel extension at the toe of the internal part of the Alpine wedge front during the Late Cretaceous–middle Eocene. This *Broken Formation* experienced an overprint of tectonic, diapiric and sedimentary processes as a result of continental collision in the late Oligocene. The NE-vergent thrusting and associated shortening produced a structurally ordered block-in-matrix fabric through mixing of both native and exotic blocks, forming the *Tectonic Mélange*. The concentration of overpressurized fluids along the thrust fault planes triggered the upward rise of shaly material, producing the *Diapiric Mélange*, which in turn provided the source material for the downslope emplacement of the youngest, late Oligocene *Sedimentary Mélange*. The Sedimentary Mélange units unconformably cover the collisional thrust faults, constraining the timing of the youngest episode of contractional deformation in the accretionary wedge. Our multi-scale structural analysis of the Ligurian accretionary wedge shows that tectonic, diapiric and sedimentary processes played a significant role in its evolution, and that the interplay between and the superposition of these different processes strongly controlled the dynamic equilibrium of the accretionary wedge in the NW Apennines–W Alps. This kind of polygenetic mélange development may be common in many modern and ancient accretionary complexes, and the processes involved in their formation are likely to be responsible for major tsunamic events in convergent margins.

59 **Key words:** accretionary wedge; polygenetic mélange; tectonic, diapiric and sedimentary  
60 processes; Northern Apennines; Tertiary Piedmont Basin.

61

## 1. Introduction

The shape and growth of the frontal wedge of the modern accretionary complexes repeatedly change to maintain the dynamic equilibrium in the wedge through alternating tectonic and sedimentary (i.e., gravitational) activities (e.g., Davis et al., 1983; Scholl et al., 1977; von Huene and Lallemand, 1990; Gutscher et al., 1998; Cliff and Vannucchi, 2004; Wang and Hu, 2006; Buiter, 2012; Gravelau et al., 2012; Haq, 2012). Highly sheared, disrupted and fragmented rock units and tectonic mélanges are the products of tectonics occurring along the basal décollements in accretionary wedges and out-of-sequence thrust-faults, and within the subduction channels (e.g., Karig and Sharman, 1975; Cloos, 1982; Moore and Byrne, 1987; Taira et al., 1992; Dileonardo et al., 2002; Collot et al., 2011). Mass-transport deposits and sedimentary mélanges result from slope instability in the trench-inner slope and in the upper parts of frontal wedges (e.g., Lallemand et al., 1990; Duperret et al., 1995; Goldfinger et al., 2000; von Huene et al., 2000; Collot et al., 2001; McAdoo et al., 2004; Sage et al., 2006; Mosher et al., 2008; Ogawa et al., 2011; Strasser et al., 2009, 2011). Shale and mud diapirism represent the upward rise of overpressured fluids migrating along the basal décollement or channeled along megasplay faults (e.g., Brown and Westbrook, 1988; Moore and Vrolijk, 1992; Kopf, 2002; Chamot-Rooke et al., 2006; Camerlenghi and Pini, 2009).

Mélanges commonly occur in ancient examples of exhumed accretionary wedges on-land, showing a complex internal block-in-matrix fabric that may vary both laterally and vertically (e.g., Maxwell, 1974; Cloos, 1984; Raymond, 1984; Cowan, 1985; Byrne and Fisher, 1990; Barnes and Korsch, 1991; Onishi and Kimura, 1995; Ogawa, 1998; Dilek et al., 1999, 2005; Pini, 1999; Dilek and Robinson, 2003; Codegone et al., 2012a, 2012b; Dilek et al., 2012;

86 Festa et al., 2010a; Ukar, 2012; Wakabayashi, 2012; Singlenton and Cloos, 2013). The  
 87 primary internal structures of mélanges and mélange-forming processes are commonly  
 88 obscured by subsequent deformational events, resulting in superposed and mixed mélanges  
 89 types, such tectonic, sedimentary and diapirc mélanges. Much effort has been made to  
 90 establish a set of useful criteria by which to distinguish mélange types in ancient accretionary  
 91 complexes (e.g., Aalto, 1981; Naylor, 1982; Raymond, 1984; Cowan, 1985; Barber et al.,  
 92 1986; Bettelli and Panini, 1989; Harris et al., 1998; Orange, 1990; Pini, 1999; Cowan and Pini,  
 93 2001; Dela Pierre et al., 2007; Yamamoto et al., 2009, 2012; Festa et al., 2010, 2012;  
 94 Vannucchi and Bettelli, 2010; Festa, 2011; Osozawa et al., 2009, 2011; Wakabayashi, 2011,  
 95 2012; Codegone et al., 2012a, 2012b). These criteria are mainly based on meso-scale  
 96 structural observations and analyses (e.g., Hsü, 1968; Cowan, 1985; Barber et al., 1986;  
 97 Lash, 1987; Orange, 1990, Pini, 1999; Bettelli and Vannucchi, 2003) and are more rarely on  
 98 map-scale or micro-scale studies (e.g., Aalto, 1981; Bettelli and Panini, 1989; Ogawa, 1998;  
 99 Pini, 1999; Alonso et al., 2006; Dela Pierre et al., 2007; Festa, 2011; Saleeby, 1979, 2011;  
 100 Wakabayashi, 2011, 2012; Hitz and Wakabayashi, 2012; Codegone et al., 2012a, Wakita,  
 101 2012; Vannucchi and Maltman, 2000; Kawamura et al., 2007; Michiguchi and Ogawa, 2011).  
 102 However, a multi-scale approach to differentiate different chaotic rock units that were formed  
 103 by different processes in accretionary wedge development has been rather limited in the  
 104 literature (see, e.g., Pini, 1999; Codegone et al., 2012a, 2012b).

105

106 In this paper, we document the internal structure, tectonostratigraphic units, and geological  
 107 evolution of the Ligurian accretionary wedge in Monferrato of the NW Apennines in Italy (Fig.  
 108 1) through multi-scale, field- and laboratory-based structural studies (from geological map-to  
 109 meso-scale and scanning electron microscope-scale) of a composite chaotic rock unit,

previously designated as an “undifferentiated chaotic complex” (e.g., Elter et al., 1966; Bonsignore et al., 1969; Dela Pierre et al., 2003a). We differentiate the occurrence of “polygenetic mélanges” that were formed by the contemporaneous to sequential operation of tectonic, diapiric and sedimentary processes that took place to maintain the dynamic equilibrium during the evolution of this accretionary wedge. This study presents, therefore, a detailed structural anatomy of an exhumed accretionary wedge, whose evolution included both subduction-accretion and collisional tectonic events during the Late Cretaceous through late Oligocene.

## 2. Regional geology

The Ligurian Units in the Northern Apennines (Fig. 1) consist of the Mesozoic to early Cenozoic sedimentary successions and the Jurassic ophiolites that collectively represent the remnants of the Ligurian Ocean (Fig. 2A; see, e.g., Marroni et al., 2001; Bortolotti et al., 2005), which evolved between European plate and the Adria microplate (i.e., Africa promontory) (e.g., Coward and Dietrich, 1989; Cavazza et al., 2004, and references therein; see also Molli et al., 2010). The Internal, External and Sub-Ligurian Units (Fig. 1; e.g., Marroni et al. 2010, and references therein) contain those tectonosedimentary assemblages that were originally deposited in an oceanic basin, in an ocean-continent transition zone (OCT), and in a rifted continental margin of Adria, respectively (Fig. 2). During the Late Cretaceous through middle Eocene and prior to the continental collision, these Units were deformed and incorporated into the Alpine accretionary wedge (i.e., Principi and Treves, 1984; Marroni et al., 2001, 2010; Bortolotti et al., 2005; Vezzani et al., 2010). Here, the Ligurian Units (i.e., part of the modern Northern Apennine) and the Western Alpine Units (i.e., modern Western Alps)



were tectonically imbricated along oppositely verging (Fig. 2B), the internal (i.e. eastern) and external (i.e. western) parts of the Alpine wedge, respectively (e.g., Roure et al., 1996; Cavazza et al., 2004; Marroni et al., 2010 and reference therein).

In the middle Eocene (Figs. 2C and 2D), the east-dipping “alpine” subduction was halted due to the partial subduction of the European continental crust (e.g., Carminati et al., 2004, Marroni et al., 2010). The establishment of a West-dipping “Apennine” subduction formed an ENE-facing accretionary wedge (i.e., the proto-Apennines involving the External Ligurian Units) and involved the subduction of the thinned Adria continental margin (Figs. 2C and 2D; e.g., Marroni et al., 2010; see also Castellarin, 1994; Carminati et al., 2004; Cavazza et al., 2004; Vignaroli et al., 2008; Molli et al., 2010; Vezzani et al., 2010). As a result, the External Ligurian Units were underthrust below the Internal Ligurian Units (Figs. 2C and 2D).

Several episutural basins (Figs. 1 and 3) that developed in the proto-Northern Apennines (i.e., Epi-ligurian Units; see, e.g., Mutti et al., 1995; Ricci Lucchi, 1986) and in the internal part of the Western Alps (i.e., *Tertiary Piedmont Basin*; see Piana and Polino, 1995; Biella et al., 1997) in the middle-late Eocene cover all the accretionary wedge assemblages and related structures.

The Monferrato and Torino Hill correspond to the northern part of the late Eocene–late Miocene *Tertiary Piedmont Basin*, representing the northernmost segment of the Northern Apennines where the External Ligurian Units (i.e., the remnants of the outer part of the Ligurian accretionary wedge) crop out (e.g., Elter et al., 1966; Dela Pierre et al., 2003a; Festa et al., 2009a). Monferrato is separated from the Torino Hill by the Rio Freddo Deformation

Zone (*sensu* Piana and Polino, 1995) (Fig. 1). Its tectono-stratigraphic evolution occurred in four main stages during the Rupelian, late Oligocene–pre late Burdigalian, late Serravallian, and Messinian (see Piana, 2000; Dela Pierre et al., 2003b, 2007; Festa et al., 2005, 2009b). During the Rupelian stage, NW-striking left-lateral transtensional faults associated with rifting of the Balearic Sea controlled the drowning of the early Oligocene shelf along a series of NW-striking pull-apart basins (Castellarin, 1994; Mutti et al., 1995). The subsequent late Oligocene–pre late Burdigalian stage was marked by the northwestward migration of the frontal thrust system of the Northern Apennines in Monferrato. Due to the E-W regional shortening, the previously formed transtensional faults were inverted into left-lateral transpressional faults, facilitating the transportation of the shelf sediments onto the slope deposits. The late Burdigalian unconformity, which overlapped these transpressional faults, was crosscut by the NE-SW-striking reverse faults, developed during the third tectonic stage in the Serravallian. Since the late Messinian, regional N-S shortening has caused the overthrusting of Monferrato and Torino Hill onto the Po Plain foredeep along the Northern Apennines frontal thrust (i.e., Padane Thrust Front in Fig. 1).

### 3. Chaotic rock units in Monferrato

In Monferrato, the exhumed Ligurian accretionary wedge consists mainly of an Upper Cretaceous–middle Eocene undifferentiated chaotic complex (i.e., “Undifferentiated complex” *sensu* Bonsignore et al., 1969; “La Pietra chaotic complex” *sensu* Dela Pierre et al., 2003a, 2003b; Festa et al., 2009a, 2009b). Sacco (1935) and then Beets (1940) made the first lithostratigraphic distinction in this chaotic complex on their geological maps. Elter et al. (1966) and Bonsignore et al. (1969) correlated part of this undifferentiated chaotic complex

182 (i.e., the “Lauriano complex” of Albian–Cenomanian age and the “Monteu da Po Flysch” of  
 183 Maastrichtian age) with the “basal complex” (i.e., *Argille varicolori* Auct. and Ostia  
 184 sandstones) and the Monte Cassio Flysch (Cassio Unit Auct.) of the External Ligurian Units of  
 185 the Northern Apennines, respectively. However, these authors did not distinguished this  
 186 succession on their geological maps.

187

188 We have mapped in detail the Western Monferrato area, differentiating a lithostratigraphic  
 189 succession that is comparable to the upper part of the Cassio Unit of the External Ligurian  
 190 Units in the Northern Apennines (Figs. 3 and 4). This succession consists of the late  
 191 Campanian(?)–Maastrichtian Monte Cassio Flysch (Fig. 3) that overlies a composite chaotic  
 192 rock unit (i.e., part of the “undifferentiated complex” of Bonsignore et al., 1969). On the basis  
 193 of its block-in-matrix fabric, macro- and micro-structural features (observed at various scales),  
 194 and the nature, age and origin of its blocks (i.e., native or exotic), we have subdivided this  
 195 composite chaotic rock unit into a broken formation and three different types of polygenetic  
 196 mélanges. Each of the polygenetic mélanges represents the superposition of tectonic, diapiric  
 197 and sedimentary processes that reworked the block-in-matrix fabric of the broken formation  
 198 and the previously formed mélange/s. The broken formation corresponds to the Upper  
 199 Cretaceous (Santonian – Campanian) *Argille varicolori* (i.e., upper part of the “basal  
 200 complex”; see Figs. 3 and 4). It represents a lithostratigraphic unit resulting from the tectonic  
 201 dismemberment of alternating shale, sandstone and manganiferous siltstone layers.

202

203 In the following, we refer to broken formation (*sensu* Hsü, 1968) a stratally disrupted unit  
 204 preserving its lithological and chronological identity (see Fig. 4) and containing only “native”  
 205 components (i.e., intraformational origin; see also Raymond, 1984; Cowan, 1985; Pini, 1999;

Festa et al., 2012 and reference therein, for a complete discussion on the terms “native” and “exotic”). On the contrary, we refer to “mélange” a body of mixed rocks, containing both “exotic” (i.e., extraformational origin) and “native” components, in a pervasively deformed matrix (see, e.g., Raymond, 1975, 1984; Silver and Beutner, 1980; Festa et al., 2012). Mélanges may be formed by tectonic, sedimentary, and intrusive processes or through the combination and superposition (i.e., polygenetic mélanges) of these processes (e.g., Raymond, 1984; Festa et al., 2010a and reference therein).

### 3.1 Broken Formation (i.e., Upper Cretaceous *Argille varicolori*)

The *Broken Formation* in Monferrato corresponds to the areally largest unit in the composite chaotic rock unit (see *Argille varicolori* in Fig. 4). At the mesoscale, its deformation is characterized by layer-parallel extension (Fig. 5A), which produced a progressive bedding-parallel boudinage of cm- to m-long blocks, which are exclusively of native origin (i.e., “intraformational”). The preferred alignment and the boudinage structures of these blocks produced a strong fabric, defining pseudo-bedding in the *Argille varicolori*. The more competent sandstone, limestone, manganiferous siltstone, calcarenite, and marly limestone rocks show a progressive stratal disruption from continuous layering to isolated, phacoidal or tabular blocks in a shaly matrix. Elongated blocks (mean long-axis: 33 cm) display a high aspect ratio (long axis/short axis) with a mean value ranging from 3.5 to 4 (Figs. 6A and 6B), and an irregular, flat- to ellipsoidal shape corresponding to different degrees of extensional shearing of the bedding plane in two orthogonal directions. Pinch-and-swell and boudinage structures are mainly asymmetric, and define a planar alignment that is consistent with extensional shearing in the ESE-WNW direction (Figs. 5A and 6C). R and R' Riedel shears crosscut the

asymmetric, elongated blocks (Fig. 5A). The boudins, on the other hand, appear symmetrical in the NNE-direction (Fig. 5A).

Decimeter-wide noncylindrical, and asymmetrical intra-layer folds occur extensively throughout the *Broken Formation* (Fig. 5B). These folds are commonly rootless and transposed, and have curvilinear axial surfaces. Their fold axes display a broad girdle with two NNE- and WNW oriented maxima (Figs. 5B and 6C). The folds are sheath-like and symmetric along NNE–SSW cross-sections (Fig. 5B), whereas their limbs are asymmetrically boudinaged by R and C' shears along ESE–WNW cross-sections.

At a hand sample scale, we observe alternating layers (mm- to cm-thick) of stretched and disrupted varicolored shale, siltstone, limestone and sandstone as a result of layer-parallel extension (Figs. 5C, 5D and 5E). The more competent sandstone and limestone layers are asymmetrically boudinaged along ENE–WNW-oriented sections (Figs. 5C and 5D). The boudins are connected to each other by elongated wisps and tails, whose alignment defines a tectonically induced, pseudo-layering that is nearly parallel to the original depositional bedding (Fig. 5D). Numerous low- to high-angle normal faults and R–R' shears crosscut the more competent rocks (Fig. 5D), and continue into the weak shaly matrix as C'-type shears (*sensu* Passchier and Trouw, 2005) with only mm-scale displacements (Fig. 5E).

At the scanning electron microscope scale, the fabric of the shaly matrix is defined by the preferred alignment of the platelets of clay minerals, defining anastomosing cleavage domains with spacing of 3 to 18  $\mu\text{m}$  (Fig. 5F). This fabric in the matrix is parallel to the bedding in the rocks, suggesting that sediments underwent burial-related flattening (uniaxial

layer-normal compression) during the early stages of their lithification. Disjunctive shear surfaces (C'-type shear *sensu* Passchier and Trouw, 2005, and R shear) crosscut this bedding-parallel fabric at low-angles (Fig. 5F). These structures affected both the pseudo-bedding planes and the fold limbs, indicating that intralayer folding and boudinage development on the fold limbs were spatially and temporally related (see also Vannucchi et al., 2003). Extensional-shear surfaces mimic the geometry of those observed at the hand sample scale (Figs. 5E and 5F).

### 3.2 Tectonic Mélange

It is characterized by a highly sheared block-in-matrix fabric (Fig. 7A) with mixed blocks of both native (e.g., limestone, sandstone and manganiferous siltstone of the *Argille varicolori*) and exotic origin. The exotic rock blocks were wrenched from the lowest stratigraphic horizons of the “basal complex” (e.g., early Cretaceous Palombini shale, Cenomanian(?)–early Campanian Scabiazza sandstone), the older buried succession (Upper Jurassic-to lower Cretaceous Maiolica limestone), the late Campanian(?)–Maastrichtian Monte Cassio Flysch, and the Upper Eocene – Oligocene *Tertiary Piedmont Basin* succession.

At the map scale (Fig. 4), the *Tectonic Mélange* defines a narrow zone (up to 50 meters wide) in the hangingwall of the NE-vergent thrust faults, emplacing the *Argille varicolori* over the Monte Cassio Flysch and the Upper Eocene–Oligocene succession of the *Tertiary Piedmont Basin*. Here, the pre-existing fabric of the *Broken Formation* is strongly overprinted and reworked by shearing associated with thrusting, forming a scale independent, “structurally ordered” block-in-matrix fabric (*sensu* Festa, 2011; see Figs. 7A and 7B). Away from the

thrust faults, the rocks gradually acquire the original, layer-parallel extensional fabric of the *Broken Formation* (Fig. 4).

At the mesoscale, the structurally ordered block-in-matrix fabric gives way to the NE-vergent (Figs. 7A and 7B) shear zones (with secondary left-lateral strike slip component of movement) caused by E-W directed regional shortening (see Figs. 6C; see also Piana, 2000; Festa et al., 2005, 2009b). The blocks in the *Tectonic Mélange* show a prevalent phacoidal shape (more rarely tabular), with mean values of their aspect ratio (long axis/short axis) ranging from 2.5 to 2.8 (Figs. 6A and 6B). Elongated blocks are imbricated in the direction of shortening and are bounded or disrupted by the anastomosing S-C shears (Figs. 7A and 7B). The exotic blocks are mixed with the native blocks derived from the *Broken Formation* along these shear zones. The long-axes of the SW-dipping native blocks (Fig. 6C) range in size from 5 cm to 90 cm with a mean length of ~20 cm (Fig. 6A). Exotic blocks are commonly larger in size (long-axis up to 125 cm, and mean length of 35 cm). The difference in size between the smaller native blocks and the larger exotic ones may be related to the nature of different processes of stratal disruption and to the thickness of the beds in the original stratigraphic succession. The mean size of the native blocks is smaller in the *Tectonic Mélange* (mean long-axis ~20 cm) than in the *Broken Formation* (mean long-axis 33 cm), indicating that the *Tectonic Mélange* developed by imposing significant tectonic strain on the earlier formed *Broken Formation*. In general, however, we observe a progressive decrease in the block size and in the intensity of tectonic mixing away from the thrust faults (Fig. 6B). This progressive decrease in the size of blocks away from the thrust faults appears to be related to the progressive decrease of mixing of native and exotic blocks.

The shaly matrix of the *Tectonic Mélange* shows a pervasive NE-vergent scaly fabric (Figs. 7B and 7C) defined by anastomosing P and R shears, which are compatible with the overall reverse sense of shearing (Fig. 6C). Interlacing of disjunctive shear surfaces and the S-C fabric elements subdivides the shaly matrix into mm- to cm-long, lozenge-shaped lenses (Figs. 7B and 7C), whose surfaces are generally well polished and smooth.

Our scanning electron microscope observations also show the evidence of a pervasive S-C fabric in the shaly matrix that defines submillimetric to millimetric, sigmoidal-shaped lenses with polished and striated surfaces. These surfaces are finely spaced (few  $\mu\text{m}$ -to tens of  $\mu\text{m}$ ) and envelope tabular, phacoidal (or rarely equidimensional), small clasts (5-20  $\mu\text{m}$  in size) that are strongly aligned with the main fabric in the rocks (Fig. 7D). This fabric is defined by the reorientation of clay particles and elongated clasts during shear deformation.

### 3.3 Diapiric Mélange

Diapiric processes reworked the block-in-matrix fabric elements of both the *Broken Formation* and the *Tectonic Mélange* of the *Argille varicolori*, forming tens to hundreds of meters-wide diapiric bodies and dm- to m-wide shaly dike injections in the hanging wall units of the main thrust faults (Figs. 4 and 8A). In the field, the subvertical block-in-matrix fabric of the diapiric intrusions makes a sharp contact against the low-angle, NW-striking and “structurally ordered” fabric of the older *Broken Formation* and the *Tectonic Mélange* (Fig. 8A). In map view, the wider diapiric bodies display a roughly rounded or an elliptical shape (Figs. 4 and 8A), characterized by the concentric juxtaposition of disrupted stratigraphic horizons wrenched from both the *Argille varicolori*, the buried “basal complex”, and the older stratigraphic



326 succession (i.e., Scabiazza sandstone, Maiolica limestone, Palombini shale, etc.; see [Fig.](#)  
327 [8B](#)). Irregularly shaped blocks of the Monte Cassio Flysch and some rare blocks of the Upper  
328 Eocene – Oligocene *Tertiary Piedmont Basin* succession also occur within the diapiric  
329 mélange.

330

331 At the mesoscale and in its type locality (located in the northern sector; see [Fig. 8A](#)), the  
332 diapiric bodies show internal structural zoning (*sensu* Orange, 1990; Dela Pierre et al., 2007;  
333 Festa, 2011). Their margins are characterized by a sub-vertical block-in-matrix fabric with  
334 mainly phacoidal (rarely tabular) blocks ([Fig. 8B](#)). The long axes of the blocks range from 20  
335 cm to 40 cm, with a mean aspect ratio (long axis/short axis) of 2.5 to 2.6 ([Figs. 6A and 6B](#)).  
336 These blocks are enveloped by a varicolored shaly matrix displaying a pervasive, vertical  
337 scaly fabric ([Fig. 6C](#)) and flame-shaped injections wrapping around the blocks ([Fig. 8C](#)). The  
338 center of the diapiric bodies shows non-cylindrical folds (isoclinal-to disharmonic) with  
339 irregular axial surfaces and subvertical fold axes ([Figs. 6C and 8A](#)). The limbs of these folds  
340 have changed progressively into boudinage and pinch-and-swell features. The shaly matrix  
341 includes meter-size and larger folds traced by the sub-vertical alignment of the fragments of  
342 disrupted beds. The blocks are commonly larger in the center of the diapiric bodies than those  
343 along the margins ranging in length from 35 cm to 90 cm, and showing a mean aspect ratio  
344 (long axis/short axis) of 2.1 to 2.3 ([Figs. 6A and 6B](#)).

345

346 Scanning electron microscope observations of the shaly matrix of the diapiric bodies reveal a  
347 sub-vertical flow fabric defined by the overall alignment of the platelets of clay minerals  
348 defining anastomosing and folded cleavage domains ([Fig. 8E](#)). Surfaces of the clay platelets  
349 do not show striations. Clay particles in the center of the diapiric bodies are commonly

deformed into isoclinal or irregular and convolute folds (fold hinges 10-20  $\mu\text{m}$  wide) with axial surfaces aligned parallel to the flow fabric (Fig. 8E). Cleavage domains drape around the rounded to irregularly shaped clasts. Only the long-axes of the clasts are aligned with the flow fabric (Fig. 8E). Similar convolute folds also occur near and along the margins of the diapiric bodies with less irregularly deformed and well aligned clay particles (Fig. 8F) forming sigmoidal domains that are crosscut and reoriented by the sub-vertical S-C fabric elements.

### 3.4 Sedimentary *mélange* (i.e., Polygenetic argillaceous breccias)

The *Sedimentary mélange*, here named “*Polygenetic argillaceous breccias*” (Figs. 3 and 4), has been distinguished from the *Argille varicolori*. It consists of a late Oligocene chaotic block-in-matrix unit. At the map scale (Fig. 4), the polygenetic argillaceous breccias consist of up to 50-m-thick, irregularly shaped chaotic mass-transport deposits with irregular shape that unconformably overlie both the External Ligurian Units (i.e., Monte Cassio Flysch and *Argille varicolori*) and the upper Eocene-Oligocene sedimentary rocks of the *Tertiary Piedmont Basin* (i.e., Monte Piano marls and Cardona Formation).

At the mesoscale (Fig. 9A), the block-in-matrix fabric of the argillaceous breccias is characterized by a highly disordered polymictic assemblage of rock clasts and blocks (1 cm to 15 cm in size) of different ages and origins. The clasts and blocks are mainly angular to rounded in shape (mean aspect ratio of the blocks: 1.5–1.7; Figs. 6A and 6B) and are randomly distributed in a brecciated shaly matrix. The blocks are of the same lithologies as those of the diapiric *mélange*, and include some material derived from the “basal complex” (i.e., *Argille varicolori*, Scabiazza sandstone, Palombini shale) and the older stratigraphic

succession (i.e., Maiolica limestone, reddish limestone) of the External Ligurian units, as well as from the Monte Cassio Flysch, and the Upper Eocene–Upper Oligocene succession of the *Tertiary Piedmont Basin* (Monte Piano marls and Cardona Formation). The shaly matrix (Fig. 9B) is typically brecciated and envelops a polymictic assemblage of sub-millimeter to cm-long, sub-angular to rounded clasts. Elongated clasts commonly display micro-faults or fractures that accommodated extensional deformation related to mass-transport movements. In the outcrop or in the hand sample, the breccias show a structureless, isotropic fabric defined by the random distribution and orientation of the clasts, dispersed in the shaly matrix (Figs. 9A, 9B and 9C).

Locally, alternating superposition of dm- to m-thick, brecciated lenticular bodies are bounded by irregular erosional surfaces and highly sheared varicolored shaly layers (Fig. 9C). This feature may have formed as a result of the repeated emplacement and superposition of minor mass-transport deposits, which demonstrate different degrees of liquefaction and variety of blocks in the shaly matrix. The extensional shearing-related features, which correspond to a narrow (up to 50 m thick) shear zone, related to the emplacement of the polygenetic argillaceous breccias, indicate direction of emplacement of the different mass-transport bodies radially away from main diapiric bodies (Fig. 10A).

In the basal part of the argillaceous breccias the fabric shows a planar anisotropy defined by the alignment of elongated blocks parallel to the extensionally sheared layers and to the erosive basal surface (Fig. 10B). This fabric is crosscut at low angles by disjunctive extensional shear surfaces (low angle Riedel shear; see Fig. 10B).

398 Scanning electron microscope observations show scale invariance with the mesoscopic fabric  
399 described above. The microscale fabric of the argillaceous breccias is characterized in part by  
400 rounded clasts (up to 250  $\mu\text{m}$ -long) randomly distributed in a brecciated matrix, which  
401 contains strongly aligned clay particles (Fig. 9D). This matrix shows discontinuous and  
402 anastomosing surfaces wrapping around the clasts (Fig. 9E) without any trace of shearing.  
403 Only the long-axes of the clasts exhibit a common planar orientation roughly parallel to the  
404 alignment of clay particles. Spacing between the clay particles varies based on the presence  
405 or absence of clasts, and may range from  $\sim 10$  to 15  $\mu\text{m}$  in domains with abundant clasts, or  
406 from 3 to 5  $\mu\text{m}$  where clasts are scarce or absent (Fig. 9E).

407

408 Close to the basal erosional contact, the microscale fabric of the argillaceous breccias  
409 consists of sheared extensional domains defined by the alignment of compacted clay particles  
410 (cleavage domains, 3 to 5  $\mu\text{m}$  spaced) that are crosscut by low-angle, C'-type shear surfaces  
411 (*sensu* Passchier and Trouw, 2005) (Fig. 10C). Clasts here are mainly elongated and aligned  
412 parallel to the basal surface.

413

414 Decimeter- to meter-wide and up to few meter-long shale dikes intrude (Figs. 4 and 8A) the  
415 polygenetic argillaceous breccias. These dikes are composed of subvertical and convoluted  
416 injections of fluidal, red and gray shale with irregular but sharp contacts (Figs. 11A, 11B and  
417 11C). Small, cusped and flame structures, up to dm-wide, and cm- to dm-long, commonly  
418 occur along the sharp contacts of the dikes, and intrude laterally into the country rocks (Fig.  
419 11B and 11D). The matrix shows a sub-vertical deformational fabric wrapping around the  
420 tabular and boudinaged blocks (cm in size), which are rotated and reoriented parallel to the

subvertical margins of these injections (Figs. 11C and 11D). Locally, the matrix displays irregular, isoclinal folds with boudinaged limbs.

The microscale fabric (SEM images) of the shale dikes shows the same characteristic, vertically oriented structures commonly seen along the margins of the diapiric bodies. A microscale fabric similar to that described from the core zone of the diapiric bodies occurs only in the wider dike injections (few dm-wide; see Figs. 11E and 11F).

#### 4. Discussion

The imprint of tectonic, sedimentary and diapiric processes is recorded at all scales (from map- to micro-scale) in the fabric of the diverse chaotic rock units recognized in the “basal complex” of the External Ligurian Units and in the *Tertiary Piedmont Basin* succession in Monferrato (Table 1). The structural relationships between these chaotic rock units provide us with an excellent opportunity to document the processes of mélange formation, their ages, and the polygenetic, time-progressive tectonic evolution of the Ligurian accretionary wedge during the Late Cretaceous through late Oligocene. In contrast to the Circum-Pacific mélanges (e.g., the Franciscan Complex in the Western Cordillera, USA) or to those metamorphic mélange units (e.g., Western Alps), in which an age-ordered stratigraphic columnar section does not convey the duality in different ages of the accretionary complex units (i.e., formational age versus accretionary age of the units; formational age of far-traveled oceanic units versus formational age of offscraped trench sediments), the mélanges we describe from Monferrato can be easily compared with other mélange occurrences all along the Ligurian accretionary wedge whose stratigraphy (see Fig. 3) is readily correlated across

the major thrust faults. Thus, the mélanges documented in this paper provide new constraints on the lateral variations (i.e., along strike) in the structural evolution of the Ligurian accretionary wedge in NW Italy.

#### **4.1. Late Cretaceous - middle Eocene tectonic stage**

The layer-parallel extensional block-in-matrix fabric of the *Broken Formation* (i.e., Upper Cretaceous *Argille varicolori*) is consistent with a large –magnitude lateral spreading that resulted in flattening (mean aspect ratio of the blocks: 3.5–4; Fig. 6B and Table 1) in two orthogonal directions in unconsolidated sediments. The mechanisms responsible for this type of deformation have been discussed extensively in the literature and are commonly interpreted as a product of tectonic flattening across the basal shear zone of accretionary wedges (e.g., Davis et al., 1983; Lash, 1987; Kimura and Mukai, 1991; Onishi and Kimura, 1995; Hashimoto and Kimura, 1999; Kusky and Bradley, 1999; Yamamoto, 2006) or gravitational sliding on the inner trench slope (e.g., Cowan, 1985; Pini, 1999). In the Northern Apennines, this deformation has been related to a shortening event which occurred in the frontal and shallower levels of the Ligurian accretionary wedge (e.g., Pini, 1999; Vannucchi and Bettelli, 2002; Bettelli and Vannucchi, 2003) in the latest stages of accretion, and prior to the continental collision (e.g., Principi and Treves, 1984; Vai and Castellarin, 1993; Marroni and Pandolfi, 1996; Pini, 1999; Bettelli and Vannucchi, 2003; Codegone et al., 2012b).

Our data and observations suggest that during the early stages of deformation, the *Argille varicolori* underwent vertical compaction due to burial (Fig. 12), which resulted in the formation of boudinage structures, in the compaction and flattening of clay particles, and the

decrease of porosity (Fig. 12B). When sediments made their way to the toe of the wedge, compressional stress and tectonic loading produced asymmetrical boudinage and R and R' shears in the more lithified layers, and C'-type shears (*sensu* Passchier and Trouw, 2005) in the shaly matrix (Fig. 12C).

The coeval development of flattened, intralayer sheath-like folds, layer-parallel extensional fabric, and asymmetric boudinage (Fig. 12C) might have resulted from the heterogeneity of deformation at the toe of the accretionary wedge (e.g., Kimura and Mukai, 1991; Onishi and Kimura, 1995; Kusky and Bradley, 1999). The undulation of the decollement surface (see Onishi and Kimura, 1995) and/or the orientation of the layers with respect to  $\sigma_1$  might have also played a role in this heterogeneous deformation (see Kusky and Bradley, 1999). Layers dipping at high angles ( $30^\circ$ - $45^\circ$ ) to  $\sigma_1$  may have experienced both brittle extension (i.e., boudinage, R-R', C' shears and low-angle extensional faulting) and ductile contraction (i.e., folding) (Fig. 12C). Thus, at the toe of an accretionary wedge (Fig. 12A) different domains can exist where layer-parallel extension develops parallel to the fold axial surfaces, and the structures can be indistinguishable from the early extensional fabric related to vertical loading (see Kusky and Bradley, 1999).

The above-described observations indicate that deformation started just after the deposition of sediments, under unconsolidated conditions, and continued throughout progressive lithification. Therefore, the age of the earliest deformation episode must have been very close to the timing of deposition (i.e., Late Cretaceous-to middle Eocene). The structures related to this earliest deformation stage have been sealed by the unconformable deposition of the

upper Eocene Monte Piano marls, which represent the base of the *Tertiary Piedmont Basin* succession (Fig. 4).

## 4.2. Late Oligocene

The layer-parallel extensional fabric of the *Broken Formation* (i.e., Upper Cretaceous *Argille varicolori*) was overprinted and reworked by NE–vergent thrusting (with secondary left-lateral strike slip component of movement) and associated shearing during the late Oligocene (Fig. 4). Thrusting and shearing collectively led to the development of a polygenetic *mélange* of a tectonic origin (i.e., *Tectonic Mélange*; Figs. 13A and 13A'), characterized by a “structurally ordered” block-in-matrix fabric that is consistent with the direction of inferred regional shortening (see Fig. 6C). This shortening event emplaced the External Ligurian Units onto the Upper Eocene–Oligocene stratigraphic units of the *Tertiary Piedmont Basin* (e.g., Piana, 2000; Dela Pierre et al., 2003b; Festa et al., 2005; 2009b; see also Fig. 6C), and resulted in the imbrication and mixing of native and exotic blocks, mainly derived from the buried Monte Cassio Flysch, the “basal complex” (i.e., Scabiazza sandstone, Palombini shale), the older lithostratigraphic units (i.e., Maiolica limestone), and minor slices of the Upper Eocene–Oligocene *Tertiary Piedmont Basin* succession. Exotic blocks offscraped from the footwall units were accreted within the thrust shear zone and mixed with native blocks derived from the earlier *Broken Formation*. The shaly varicolored matrix facilitated the concentration of shearing deformation (i.e., pervasive scaly fabric and S-C shears), and together with fluid focused along the fault surface helped the mobilization of hard blocks and mixing processes (Figs. 13A and 13A'). The smaller size of native blocks in the *Tectonic Mélange* (mean long-axis 20 cm) with respect to those in the *Broken Formation* (mean long-axis 33 cm) shows that



the magnitude of the tectonic strain during this thrusting event was significant. The gradual transition from the *Tectonic Mélange* to the *Broken Formation*, as evidenced by decreasing of both shear deformation and the occurrence of exotic blocks far from the thrust surface, shows that the fault zone was not bounded by a sharp tectonic contact on top. The shaly matrix accommodated thrust-related deformation along a series of several dm-thick shear zones and a pervasive scaly fabric, rather than concentrating the deformation in subparallel major thrust faults bounding the *Tectonic Mélange*.

The *Tectonic Mélange* differs from those ones occurring in typical subduction (e.g., Circum-Pacific region) or collisional (e.g., Western Alps) settings where exotic blocks commonly derived from a long-subducted footwall and/or by return flow (e.g., flow mélanges of Cloos, 1982). Our *Tectonic Mélange*, that formed at shallow structural levels within the accretionary wedge, provides another example in supporting that mélanges formed directly by tectonic processes correspond to tectonic units structurally equivalent to mappable fault zones (see Cowan, 1974; Festa et al., 2010a). For example, in fact, the block-in-matrix fabric of the San Andreas fault (California) at depth, observed through drill cores, has been compared with those of tectonic mélanges (see Bradbury et al., 2011).

Because of the low permeability of the *Argille varicolori*, fluids concentrated along both thrust faults and micron- to mm-scale scaly cleavage surfaces reached the overpressure conditions, which are required to facilitate shale diapirism (e.g., Collison, 1994; Maltman, 1994; Festa, 2011, Codegone et al., 2012b; see [Fig. 13B](#)). Then, overpressurized sediments exceeding the hydrostatic pressure started rising upward and formed the diapiric injections. The difference in the velocity gradient of the upward rising shaly material (acting as a viscous fluid), increasing

from the margins toward the core of the shale diapirs, produced an internal zoning within the diapiric bodies (Fig. 8A) (e.g., Komar, 1972; Bishop, 1978; Orange, 1990; Dela Pierre et al., 2007; Festa, 2011). This process resulted in: (i) the distribution of small phacoidal blocks (long-axis length: 20 to 40 cm; mean aspect ratio: 2.5-2.6; Figs. 6A, 6B and Table 1) along the margins of the diapiric bodies, and in their preferred alignment with the intrusive contacts; and (ii) the irregular distribution of larger, irregularly shaped blocks (long-axis length: 35 to 90 cm; mean aspect ratio: 2.1-2.3; Figs. 6A, 6B and Table 1) and the formation of irregular folds with steeply plunging axes in the cores of these diapirs. The flow fabric, as observed on the scanning electron microscope images of the samples from the cores of the diapirs (Fig. 8E), is consistent with the occurrence of overpressurized fluids without shearing. On the contrary, shearing-induced structural fabric characterizes the internal architecture of the marginal zones of the diapiric bodies (Fig. 8F).

Extrusion of the diapiric bodies on the seafloor formed topographic highs (Fig. 13B), causing the downslope mobilization of unconsolidated sediments and promoting local mass-transport movements (Fig. 13C and 13C'). These mass-transport deposits were locally augmented by the extruded diapiric material (Figs. 13C and 13C'), as evidenced by the occurrence of the same exotic and native blocks in both the diapiric and sedimentary *mélanges* (*Polygenetic argillaceous breccias*). Both the radial direction of extensional shearing at the base of the polygenetic argillaceous breccias and the distribution of mass-transport bodies with respect to the main diapiric bodies (Fig. 10A) are consistent with the role of diapirism in providing the source material for the emplacement of mass-transport chaotic deposits (see also Barber et al., 1986; Barber and Brown, 1988; Barber, 2013). Although, this role is well documented in modern accretionary prisms (see, e.g., Camerlenghi and Pini, 2009 and reference therein);

564 rarely has it been documented from ancient examples (see Barber, 2013 and reference  
 565 therein). The *Sedimentary mélanges* in Monferrato unconformably overlie and cover the thrust  
 566 fault, which was responsible for the emplacement of the External Ligurian Units on the upper  
 567 Eocene–Oligocene *Tertiary Piedmont Basin* succession. These spatial and temporal  
 568 relationships constrain the timing of the emplacement of the mass-transport chaotic deposits  
 569 as the late Oligocene (Fig. 4).

570  
 571 The occurrence, at all scales, of the sheared extensional fabric at the base of these mass-  
 572 transport chaotic deposits (Fig. 10B) and its passing upward to a random distribution of  
 573 rounded and irregular blocks in a brecciated matrix (Figs. 9A and 9B) is consistent with the  
 574 mode of debris flow and mud flow processes (e.g., Pini et al., 2012). These processes were  
 575 able to disaggregate, mix and reorient the fabric of the source material in the *Diapiric Mélange*  
 576 as also supported by the smaller size of hard blocks of the *Sedimentary Mélange* with respect  
 577 to that of the *Diapiric Mélange*.

578  
 579 The occurrence of small-scale shale dike injections piercing through the Upper Oligocene  
 580 *Polygenetic argillaceous breccias* suggests that the upward rise of overpressured fluids  
 581 locally continued during and/or after the formation of these breccias (Figs. 13C' and 13C'').  
 582 These shale dikes have also been documented in the Northern Apennines (Codegone et al.,  
 583 2012b) where, however, different causative links have been documented between tectonic,  
 584 sedimentary and diapiric processes, supporting that the structural and morphological  
 585 reconstruction of the Ligurian accretionary wedge was highly dynamic and varied along strike.  
 586 The combined effect of sedimentary loading provided by the early post-emplacement of the  
 587 *polygenetic argillaceous breccias* (i.e., dissipation of internal fluid overpressure) and the

discharge of fluids after the faulting stage was responsible for the emplacement of these small dike injections. It is difficult to make these observations at the same scale (meters to tens of meters) in mass-transport deposits in modern accretionary wedges because these types of overpressured fluid features (i.e., shale dike injections) are below the standard resolution of geophysical investigations. However, the documentation of a new, overpressurized fluid supply following the emplacement of a *Sedimentary Mélange* may provide important information on the preconditioning factors that may induce downslope remobilization of the previously formed mass-transport deposits or sedimentary mélanges in modern accretionary wedges. Such remobilization may trigger major tsunami events, and hence they are potentially highly dangerous (see Kawamura et al., 2012).

## 5. Conclusions

The Late Cretaceous–late Oligocene Ligurian chaotic deposits exposed in Monferrato (NW Italy) represent an ancient analogue of a modern convergent margin accretionary wedge. This exhumed accretionary wedge includes a composite chaotic unit, known as the Upper Cretaceous *Argille varicolori*, and *Tectonic*, *Diapiric* and *Sedimentary Mélanges*. The youngest, *Sedimentary Mélange* is a result of the late Oligocene gravitational reworking of the previously formed mélanges. All these chaotic deposits and mélanges display a record of the mutual causative links among tectonic, diapiric and sedimentary processes that controlled the dynamic equilibrium of the wedge through time.

A gradual transition from homogeneous to heterogeneous deformation occurred at the toe of the accretionary wedge in the Late Cretaceous through middle Eocene, following the

deposition of the Upper Cretaceous *Argille varicolori*. The stratal disruption of this unit produced the *Broken Formation* with increased shearing. The frontal part of the wedge was subject to high instability during and after the continental collision in the late Oligocene. Out-of-sequence thrusting (with a secondary strike-slip component of movement) in the inner wedge formed the polygenetic *Tectonic Mélange*, and facilitated the mixing of exotic blocks with the *Broken Formation*. The increase of fluid pressure along the thrust faults created overpressurized hydraulic conditions triggering diapiric processes, which caused the reworking of the previously formed *Broken Formation* and *Tectonic Mélange*. This event developed the *Diapiric Mélange*. The downslope mobilization of unconsolidated, diapiric material produced the late Oligocene *Sedimentary Mélange*. These chaotic deposits of the *Sedimentary Mélange* sealed the out-of-sequence thrust faults and marked the end of *mélange* formation within the Ligurian accretionary wedge.

Our findings from the Late Cretaceous–late Oligocene chaotic deposits in Monferrato show that the frontal wedge of an accretionary complex may evolve through a combination of tectonic, diapiric and sedimentary processes that commonly overlap in time and space. Studying and documenting the mode and time of these processes in both modern and ancient examples of accretionary wedges is highly important and relevant in order for us to better understand how the gravitational instability and tectonic processes in these convergent margin products may lead to tsunamic events.

## Acknowledgments

We thank the Science Editor Christian Koeberl for his careful editorial handling. We would like to express our sincere thanks to Associate Editor Enrico Tavarnelli and Referee John Wakabayashi for their constructive and thorough reviews, and useful comments from which

we have benefited greatly in revising our manuscript. We thank also F. Coscarelli, F. Dela Pierre, G. Fioraso, E. Malerba, P. Mosca and F. Piana for passionate discussions on the Ligurian Units in Monferrato.

## References

- Aalto, K.R., 1981, Multistage melange formation in the Franciscan Complex, northernmost California: *Geology*, v. 9, p. 602–607.
- Alonso, J.L., Marcos, A., and Suárez, A., 2006, Structure and organization of the Porma mélange: progressive denudation of a submarine nappe toe by gravitational collapse, *American Journal of Science*, v. 306, p. 32–65.
- Barber, T., 2013, Mud diapirism: The origin of mélanges: cautionary tales from Indonesia: *Journal of Asian Earth Sciences*, early on line, <http://dx.doi.org/10.1016/j.jseaes.2012.12.021>.
- Barber, T., and Brown, K., 1988, Mud diapirism: The origin of melanges in accretionary complexes?: *Geology Today*, v. 4, p. 89–94.
- Barber, A.J., Tjokrosapoetro, S., and Charlton, T.R., 1986, Mud volcanoes, shale diapirs, wrench faults, and melanges in accretionary complexes, Eastern Indonesia: *American Association of Petroleum Geologists Bulletin*, v. 70, no. 11, p. 1729–1741.
- Barnes, P.M., and Korsch, R.J., 1991, Mélange and related structures in Torlesse accretionary wedge, Wairarapa, New Zealand: *New Zealand Journal of Geology and Geophysics*, v. 34, p.517–532.
- Beets, C., 1940, Die Geologie des Westlichen Teiles der Berge von Monferrato zwischen Turin und Murinsengo. Ein Beitrag Zur Geologie des Nortapennis: *Leidsche Geologische Mededeelingen*, v. 12, p. 195–250.
- Bello, M., and Fantoni, R., 2002, Deep oil play in Po Valley: Deformation and hydrocarbon generation in a deformed foreland,. In: *Deformation history, fluid flow reconstruction and reservoir appraisal in foreland fold and thrust belts: American Association of Petroleum Geologists, Hedberg Conference*, 1–4.
- Bettelli, G., and Panini, F., 1989, I mélanges dell’Appennino settentrionale tra il T. Tresinaro ed il T. Sillaro: *Memorie della Società Geologica Italiana*, v. 39, p. 187–214.
- Bettelli, G., and Vannucchi, P., 2003, Structural style of the offscraped Ligurian oceanic sequences of the Northern Apennines: new hypothesis concerning the development of mélange block-in-matrix fabric: *Journal of Structural Geology*, v. 25, p. 371–388.
- Biella, G., Polino, R., de Franco, R., Rossi, P.M., Clari, P., Corsi, A., and Gelati, R., 1997, The crustal structure of the Western Po Plain: reconstruction from integrated geological and seismic data: *Terra Nova*, v. 9, p. 28–31.
- Bigi, G., Cosentino, D., Parotto, M., Sartori, R., and Scandone, P., 1983, Structural Model of Italy: Geodynamic project, C.N.R., S.El.Ca. Firenze, scale 1:500,000, 9 sheets.

- Bishop, R.S., 1978, Mechanism for emplacement of piercement diapirs: American Association of Petroleum Geologists Bulletin, v. 62, p. 1561–1583.
- Bonsignore, G., Bortolami, G., Elter, G., Montrasio, A., Petrucci, F., Ragni, U., Sacchi, R., Sturani, C., and Zanella, E., 1969, Note Illustrative dei Fogli 56-57, Torino-Vercelli della Carta Geologica d'Italia alla scala 1:100,000: Servizio Geologico d'Italia, Roma, 96 p.
- Bortolotti, V., Marroni, M., Pandolfi, L., and Principi, G., 2005, Mesozoic to Tertiary tectonic history of the Mirdita ophiolites, northern Albania: Island Arc, v. 14, p. 471–493.
- Bradbury, K.M., Evans, J.P., Chester, J.S., Chester, F.M., and Kirschner, D.L., 2012, Lithology and internal structure of the San Andreas fault at depth based on characterization of Phase 3 whole-rock core in the San Andreas Fault Observatory at Depth (SAFOD) borehole: Earth and Planetary Science Letters, v. 310, p. 131–144.
- Brown, K.M., 1990, The nature and hydrogeologic significance of mud diapirs and diatremes for accretionary systems: Journal of Geophysical Research, v. 95, p. 8969–8982.
- Brown, K.M., and Westbrook, G.K., 1988, Mud diapirism and subcretion in the Barbados ridge accretionary complex: The role of fluids in the accretionary processes: Tectonics, v. 7, p. 613–640.
- Buiter, S.J.H., 2012, A review of brittle compressional wedge models: Tectonophysics, v. 530–531, p. 1–17.
- Byrne, T., and Fisher, D., 1990, Evidence for a weak overpressured décollement beneath sediment-dominated accretionary prisms: Journal of Geophysical Research, v. 95, B6, p. 9081–9097.
- Camerlenghi, A., and Pini, G.A., 2009, Mud volcanoes, olistostromes and Argille scagliose in the Mediterranean region: Sedimentology, v. 56, p. 319–365.
- Carminati, E., Doglioni, C., and Scrocca, D., 2004, Alps vs Apennine, *in* Crescenti, U., D'offizi, S., Merlino, S., and Sacchi, L., eds., Geology of Italy: Special volume of the Italian Geological Society for the IGC 32 Florence-2004, p. 141–152.
- Castellarin, A., 1994, Strutturazione eo-mesoalpina dell'Appennino Settentrionale attorno al “nodo ligure”, *in* Capozzi, R., and Castellarin, A., eds., Studi preliminari all'acquisizione dati del profilo CROP 1–1A La Spezia–Alpi orientali: Studi Geologici Camerti, Volume Speciale 1992/2, Camerino, Università degli Studi di Camerino, p. 99–108.
- Cavazza, W., Roure, F., and Ziegler, P.A., 2004, The Mediterranean area and the surrounding regions: active processes, remnants of former Tethyan oceans and related thrust belts, *in* Cavazza, W., Roure, F., Spakman, W., Stampfli, G.M., and Ziegler, P.A., eds., The TRANSMED Atlas: The Mediterranean Region from crust to mantle: Springer, p. 1–29.
- Chamot-Rooke, N., Rabaute, A., and Kreemer, C., 2006, Western Mediterranean Ridge mud belt correlates with active shear strain at the prism-backstop geological contact: Geology, 33, p. 861–864.
- Clift, P., and Vannucchi, P., 2004, Controls on tectonic accretion versus erosion in subduction zones: Implications for the origin and recycling of the continental crust: Reviews of Geophysics, v. 42, RG2001, doi:10.1029/2003RG000127.

- Cloos, M., 1982, Flow melanges: Numerical modeling and geologic constraints on their origin in the Franciscan subduction complex, California: Geological Society of America Bulletin, v. 93, p. 330–345.
- Cloos, M., 1984, Flow mélanges and structural evolution of accretionary wedges, *in* Raymond L.A., ed., Mélanges: their nature, origin and significance: Geological Society of America Special Paper 198, p. 71-79.
- Codegone, G., Festa, A., and Dilek, Y., 2012a, Formation of Taconic mélanges and Broken formations in the Hamburg Klippe, Central Appalachian orogenic belt, Eastern Pennsylvania: Tectonophysics, v. 568-569, p. 215-229. doi:10.1016/j.tecto.2012.03.017
- Codegone, G., Festa, A., Dilek, Y., and Pini, G.A., 2012b, Small-scale Polygenetic mélanges in the Ligurian accretionary complex, Northern Apennines, Italy, and the role of shale diapirism in superposed mélange evolution in orogenic belts: Tectonophysics, v. 568-569, p. 170-184. doi:10.1016/j.tecto.2012.02.003
- Collison, J., 1994, Sedimentary deformational structures, *in* Maltman, A., ed., The geological deformation of sediments: Chapman & Hall, London, p. 96–125.
- Collot, J.-Y., Lewis, K., Lamrche, G., and Lallemand, S. 2001, The giant Ruatoria debris avalanche on the northern Hikurangi margin, New Zealand: Result of oblique seamount subduction: Journal of Geophysical Research, v. 106, B9, p. 19271-19297.
- Collot, J.-Y., Ribodetti, A., Agudelo, W., and Sage, F., 2011, The South Ecuador subduction channel: Evidence for a dynamic mega-shear zone from 2D fine-scale seismic reflection imaging and implications for material transfer: Journal of Geophysical Research, v. 116, B11102, doi:10.1029/2011JB008429.
- Cowan, D.S., 1974, Deformation and metamorphism of the Franciscan Subduction Zone Complex northwest of Pacheco Pass, California. Geological Society of America Bulletin: v. 85, p. 1623–1634.
- Cowan, D.S., 1985, Structural styles in Mesozoic and Cenozoic mélanges in the western Cordillera of North America: Geological Society of America Bulletin, v. 96, p. 451-462.
- Cowan, D.S., and Pini, G.A., 2001, Disrupted and chaotic rock units in the Apennines, *in* Vai, G.B., and Martini, I.P., eds., Anatomy of a Mountain Belt: The Apennines and Adjacent Mediterranean Basins: Kluwer Academic Publishers, Dordrecht, p. 165-176.
- Coward, M.P., and Dietrich, D., 1989, Alpine tectonics - an overview, *in* Coward, M.P., Dietrich, D., and Park, R.G., eds., Alpine tectonics: Geological Society London Special Publications 45, p. 1–29.
- Davis, D., Suppe, J., and Dahlen, F.A., 1983, Mechanics of fold-and-thrust belts and accretionary wedges: Journal of Geophysical Research, v. 88, p. 1153-1172.
- Dela Pierre, F., Festa, A., and Irace, A., 2007, Interaction of tectonic, sedimentary and diapiric processes in the origin of chaotic sediments: an example from the Messinian of the Torino Hill (Tertiary Piedmont Basin, NW Italy): Geological Society of America Bulletin, v. 119, 1107-1119.



- Dela Pierre, F., Piana, F., Boano, P., Fioraso, G., and Forno, M.G., 2003a, Carta Geologica d'Italia alla scala 1:50,000 – Foglio 157 “Trino”: ISPRA, Istituto Superiore per la Protezione e Ricerca Ambientale. Ed. Litografia Geda, Nichelino, 1 Sheet.
- Dela Pierre, F., Piana, F., Fioraso, G., Boano, P., Bicchi, E., Forno, M.G., Violanti, D., Clari, P., and Polino, R., 2003b, Note Illustrative della Carta Geologica d'Italia alla scala 1:50,000. Foglio 157 “Trino”: APAT, Dipartimento Difesa del Suolo, 147 p.
- Dilek, Y., Thy, P., Hacker, B., and Grundvig, S., 1999, Structure and petrology of Tauride ophiolites and mafic dike intrusions (Turkey): implications for the Neotethyan ocean: *Geological Society of America Bulletin*, v. 111, p. 1192–1216.
- Dilek, Y. and Robinson, P.T., 2003. Ophiolites in Earth history: Introduction, *in* Dilek, Y. and Robinson, P.T. (Eds.), *Ophiolites in Earth History: Geological Society of London Special Publications*, vol. 218, p. 1-8.
- Dilek, Y., Shallo, M., and Furnes, H., 2005. Rift-drift, seafloor spreading, and subduction zone tectonics of Albanian ophiolites: *International Geology Review*, v. 47, p. 147–176.
- Dilek, Y., Festa, A., Ogawa, Y., and Pini, G.A., 2012, Chaos and geodynamics: Mélanges, Mélange-forming processes and their significance in the geological record: *Tectonophysics*, v. 568-569, p. 1-6.
- Dileonardo, C.G., Moore, J.C., Nissen, S., and Bangs, N., 2002, Control of internal structure and fluid-migration pathways within the Barbados Ridge décollement zone by strike-slip faulting: Evidence from coherence and three-dimensional seismic amplitude imaging: *Geological Society of America Bulletin*, v. 114, p. 51–63.
- Duperret, A., Bourgois, J., Lagabriele, Y., and Suess, E., 1995, Slope instabilities at an active continental margin: Large-scale polyphase submarine slides along the northern Peruvian margin, between 5°S and 6°S: *Marine Geology*, v. 122, p. 303–328, doi:10.1016/0025-3227(94)00125-5.
- Elter, G., Elter, P., Sturani, C., and Weidmann, M., 1966, Sur la prolongation du domaine ligure de l'Apennin dans le Monferrat et les Alpes et sur l'origine de la Nappe de la Simme s.l. des Préalpes romandes et chablaisannes: *Archives des Sciences de Genève*, v. 19, p. 279-377.
- Festa, A., 2011, Tectonic, sedimentary, and diapiric formation of the Messinian mélange: Tertiary Piedmont Basin (northwestern Italy), *in* Wakabayashi, J., and Dilek, Y., eds., *Mélanges: Processes of formation and societal significance: Geological Society of America Special Paper* 480, p. 215-232. doi: 10.1130/2011.2480(10).
- Festa, A., Boano, P., Irace, A., Lucchesi, S., Forno, M.G., Dela Pierre, F., Fioraso, G., and Piana, F., 2009a, Carta Geologica d'Italia alla scala 1:50,000. Foglio 156 “Torino Est”. ISPRA, Istituto Superiore per la Protezione e Ricerca Ambientale. Ed. Litografia Geda, Nichelino, 1 Sheet.
- Festa, A., Dela Pierre, F., Irace A., Piana F., Fioraso G., Lucchesi S., Boano P., and Forno M.G., 2009b, Note Illustrative della Carta Geologica d'Italia alla scala 1:50,000. Foglio 156 “Torino Est”: ISPRA, Istituto Superiore per la Protezione e la Ricerca Ambientale, Litografia Geda, Nichelino, p. 143.

- Festa, A., Dilek, Y., Pini, G.A., Codegone, G., and Ogata, K., 2012, Mechanisms and processes of stratal disruption and mixing in the development of mélanges and broken formations: Redefining and classifying mélanges: *Tectonophysics*, v. 568-569, p. 7-24. doi:10.1016/j.tecto.2012.05.021
- Festa, A., Piana, F., Dela Pierre, F., Malusà, M.G., Mosca, P., and Polino, R., 2005, Oligocene-Neogene kinematic constraints in the retroforeland basin of the Northwestern Alps: *Rendiconti della Società Geologica Italiana (nuova serie)*, v. 1, p. 107-108.
- Festa, A., Pini, G.A., Dilek, Y., and Codegone, G., 2010a, Mélanges and mélange-forming processes: a historical overview and new concepts: *in* Dilek, Y., ed., *Alpine Concept in Geology: International Geology Review*, v. 52, nos. 10-12, p. 1040-1105. doi: 10.1080/00206810903557704.
- Festa, A., Pini, G.A., Dilek, Y., Codegone, G., Vezzani, L., Ghisetti, F., Lucente, C.C., and Ogata, K., 2010b, Peri-Adriatic mélanges and their evolution in the Tethyan realm, *in* Dilek, Y., ed., *Eastern Mediterranean geodynamics (Part II): International Geology Review*, v. 52, nos. 4-6), p. 369-406. doi: 10.1080/00206810902949886.
- Goldfinger, C., Kulm, L.D., McNeill, L.C., and Watts, P., 2000, Super-scale failure of the southern Oregon Cascadia margin: *Pure and Applied Geophysics*, v. 157, p. 1189–1226, doi: 10.1007/s000240050023.
- Gravelau, F., Malavieille, J., and Dominguez, S., 2012, Experimental modeling of orogenic wedges: a review: *Tectonophysics*, v. 538-540, p. 1-66.
- Gutscher, M.A., Kukowski, N., Malavieille, J., and Lallemand, S., 1998, Episodic imbricate thrusting and underthrusting: Analog experiments and mechanical analysis applied to the Alaskan accretionary wedge: *Journal of Geophysical Research*, v. 103, B5, 10, p.161–10,176, doi:10.1029/97JB03541.
- Haq, S.S.B., 2012, Out-of-sequence thrusting in experimental Coulomb wedges: implications for the structural development of mega-spaly and forearc basins: *Geophysical Research Letters*, v. 39, L20306, doi: 10.1029/2012GL053176
- Harris, R.A., Sawyer, R.K., and Audley-Charles, M.G., 1998, Collisional melange development: geologic associations of active melange-forming processes with exhumed melange facies in the western Banda orogen, Indonesia: *Tectonics*, v. 17, n. 3, p. 458-479.
- Hashimoto, Y., and Kimura, G., 1999, Underplating process from mélange formation to duplexing: Example from the Cretaceous Shimanto Belt, Kii Peninsula, southwest Japan: *Tectonics*, v. 18, p. 92–107.
- Hitz, B., and Wakabayashi, J., 2012, Unmetamorphosed sedimentary mélange with high-pressure metamorphic blocks in a nascent forearc basin setting: *Tectonophysics*, v. 568-569, p. 124-134.
- Hsü, K.J., 1968, Principles of mélanges and their bearing on the Franciscan-Knoxville Paradox: *Geological Society of America Bulletin*, v. 79, p. 1063–1074.
- Karig, D.E., and Sharman, G., 1975, Accretion and subduction in Pacific trenches: *Geological Society of America Bulletin*, v. 86, p. 377-389.

- Kawamura, K., Ogawa, Y., Oyagi, N., Kitahara, T., and Anma, R., 2007, Structural and fabric analyses of basal slip zone of the Jin'nosuke-dani landslide, northern central Japan: its application to the slip mechanism of decollement: *Landslides*, v. 4, p. 371-380.
- Kawamura, K., Sasaki, T., Kanamatsu, Y., Sakaguchi, A., Ogawa, Y., 2012, Large submarine landslides in the Japan Trench: A new scenario for additional tsunami generation: *Geophysical Research Letters*, v. 39, doi: 10.1029/2011GL050661.
- Kimura, G., and Mukai, A., 1991, Underplated units in an accretionary complex: melange of the Shimanto belt of eastern Shikoku, southwest Japan: *Tectonics*, v. 10, n. 1, p. 31-50.
- Komar, P.D., 1972, Flow differentiation in igneous dikes and sills: Profiles of velocity and phenocryst concentration: *Geological Society of America Bulletin*, v. 83, p. 3443-3448.
- Kopf, A., 2002, Significance of mud volcanism: *Reviews of Geophysics*, v. 40, p. 1-51.
- Kusky, T.M., and Bradley, D.C., 1999, Kinematic analysis of melange fabrics: examples and applications from the McHugh Complex, Kenai Peninsula, Alaska: *Journal of Structural Geology*, v. 21, p. 1773-1796.
- Lallemand, S., Collot, J.Y., Pelletier, B., Rangin, C., and Cadet, J.P., 1990, Impact of oceanic asperities on the tectonogenesis of modern convergent margins: *Oceanologica Acta*, v. 10, p. 17-30.
- Lash, G.G., 1987, Diverse melanges of an ancient subduction complex: *Geology*, v. 15, p. 652-655.
- Maltman, A., 1994, Introduction and overview, *in* Maltman, A., ed.: *The geological deformation of sediments*. Chapman & Hall, London, p. 1-35.
- Marroni, M., and Pandolfi, L., 1996, The deformation history of an accreted ophiolite sequence: The internal Liguride units (northern Apennines, Italy): *Geodinamica Acta*, v. 9, p. 13-29.
- Marroni, M., and Pandolfi, L., 2007, The architecture of an incipient oceanic basin: a tentative reconstruction of the Jurassic Liguria-Piemonte basin along the Northern Apennines-Alpine Corsica transect: *International Journal of Earth Sciences*, v. 96, p. 1059-1078.
- Marroni, M., Meneghini, F., and Pandolfi, L., 2010, Anatomy of the Ligure-Piemontese subduction system: evidence from Late Cretaceous-middle Eocene convergent margin deposits in the Northern Apennines, Italy: *International Geology Review*, v. 52, p. 1160-1192.
- Marroni, M., Molli, G., Ottria, G., and Pandolfi, L., 2001, Tectono-sedimentary evolution of the External Liguride units (Northern Apennines, Italy): insight in the pre-collisional history of a fossil ocean-continent transition zone: *Geodinamica Acta*, v. 14, p. 307-320.
- Maxwell, J.C., 1974, Anatomy of an orogeny: *Geological Society of America Bulletin*, v. 85, p. 1195-1204.
- McAdoo, B.G., Capone, M.K., and Minder, K., 2004, Seafloor geomorphology of convergent margins: Implications for Cascadia seismic hazard: *Tectonics*, v. 23, TC6008, doi:10.1029/2003TC001570.

- Michiguchi, Y., and Ogawa, Y., 2011, Implication of dark bands in Miocene–Pliocene accretionary prism, Boso Peninsula, central Japan, *in* Wakabayashi, J., and Dilek, Y., eds., *Melanges: Processes of formation and societal significance: Geological Society of America Special Papers* 480, p. 247–260.
- Moore, J.C., and Byrne, T., 1987, Thickening of fault zones: A mechanism of melange formation in accreting sediments: *Geology*, v. 15, p. 1040–1043.
- Moore, J.C., and Vrolijk, P., 1992, Fluids in accretionary prisms: *Reviews of Geophysics*, v. 30, no. 2), p. 113–135.
- Molli, G., Crispini, L., Malusà, G.M., Mosca, P., Piana, F., and Federico, L., 2010, Geology of the Western Alps – Northern Apennines junction area: a regional review: *Journal of Virtual Explorer*, v. 36, no. 10, doi: 10.3809/jvirtex.2010.00215
- Mosca, P., Polino, R., Rogledi, S., and Rossi, M., 2010, New data for the kinematic interpretation of the Alps–Apennines junction (Northwestern Italy): *International Journal of Earth Science*, v. 99, no. 4, p. 833–849.
- Mosher, D.C., Austin, J.A., Jr., Fisher, D., and Gulick, S.P., 2008, Deformation of the northern Sumatra accretionary prism from high-resolution seismic reflection profiles and ROV observations: *Marine Geology*, v. 252, p. 89–99, doi:10.1016/j.margeo.2008.03.014.
- Mutti, E., Papani, L., di Biase, D., Davoli, G., Mora, S., Degadelli, S., and Tinterri, R., 1995, Il bacino terziario epimesoalpino e le sue implicazioni sui rapporti tra Alpi e Appennino: *Memorie della Società Geologica*, v. 47, p. 217–244.
- Naylor, M.A., 1982, The Casanova Complex of the Northern Apennines: A mélange formed on a distal passive continental margin: *Journal of Structural Geology*, v. 4, p. 1–18.
- Ogawa, Y., 1998, Tectonostratigraphy of the Glen App area, Southern Uplands, Scotland: anatomy of Ordovician accretionary complex: *Journal of the Geological Society of London*, v. 155, p. 651–662.
- Ogawa, Y., Anma, R., and Dilek, Y., 2011, Accretionary prism and convergent margin tectonics in the Northwest Pacific Basin. *Book Series in Modern Approaches in Solid Earth Sciences*, Springer Science+Business Media B.V. 2011Springer Science, Dordrecht, The Netherlands. ISBN 978-90-481-884-0.
- Onishi, C.T., and Kimura, G., 1995, Change in fabric of mélange in the Shimanto Belt, Japan: Change in relative convergence?: *Tectonics*, v. 14, p. 1273–1289.
- Orange, D.L., 1990, Criteria helpful in recognizing shear-zone and diapiric mélanges: examples from the Hoh accretionary complex, Olympic Peninsula, Washington: *Geological Society of America Bulletin*, v. 102, p. 935–951.
- Osozawa S., Morimoto J., and Flower F.J., 2009, “Block-in-matrix” fabrics that lack shearing but possess composite cleavage planes: A sedimentary mélange origin for the Yuwan accretionary complex in the Ryukyu island arc, Japan: *Geological Society of America Bulletin*, v. 121, p. 1190–1203.

- Osozawa S., Pavlis T., and Flowers M.F.J., 2011, Sedimentary block-in-matrix fabric affected by tectonic shear, Miocene Nabae complex, Japan, *in* Wakabayashi, J., and Dilek, Y., eds., *Mélanges: Processes of Formation and Societal Significance*: Geological Society of America Special Paper 480, p. 189-206. doi: 10.1130/2011.2480(08)
- Passchier, C.W., and Trouw, R.A., 2005, *Microtectonics*: Springer, Berlin - Heidelberg - New York, 365 p.
- Piana, F., 2000., Structural features of Western Monferrato (Alps-Appennines junction zone, NW Italy): *Tectonics*, v. 19, p. 943-960.
- Piana, F., and Polino, R., 1995, Tertiary structural relationships between Alps and Apennines: The critical Torino Hill and Monferrato area: *Northwestern Italy: Terra Nova*, v. 7, p. 138–143.
- Pini, G.A., 1999, Tectonosomes and olistostromes in the Argille Scagliose of the Northern Apennines, Italy: *Geological Society of America Special Paper* 335, 73 p.
- Pini, G.A., Ogata, K., Camerlenghi, A., Festa, A., Lucente, C.C., and Codegone, G., 2012, Sedimentary mélanges and fossil mass-transport complexes: a key for better understanding submarine mass movements?, *in* Yamada, Y., et al., eds., *Submarine mass movements and their consequences: Advances in natural and technological hazards research*, 31: Springer Science+Business Media B.V., p. 585–594.
- Principi, G., and Treves, B., 1984, Il sistema Corso-Appenninico come prisma di accrezione. Riflessi sul problema generale del limite Alpi-Appennini: *Memorie della Società Geologica Italiana*, v. 28, p. 549-576.
- Raymond, L.A., 1975, Tectonite and mélange - a distinction: *Geology*, v. 3, p. 7–9.
- Raymond, L.A., 1984, Classification of mélanges, *in* Raymond L.A., ed., *Mélanges: their nature, origin and significance*: Geological Society of America Special Paper 198, p. 7-20.
- Remitti, F., Vannucchi, P., Bettelli, G., Fantoni, L., Panini, F., and Vescovi, P., 2011, Tectonic and sedimentary evolution of the frontal part of an ancient subduction complex at the transition from accretion to erosion: the case of the Ligurian wedge of the northern Apennines, Italy: *Geological Society of America Bulletin*, v. 123, n. 1-2, p. 51-70.
- Ricci Lucchi, F., 1986, The Oligocene to recent foreland basin of the Northern Apennines, *in* Allen, P.A., and Homewood, P., eds., *Foreland basins*: International Association of Sedimentologists, Special Publication, v. 8, p. 105–139.
- Roure, F., Bergerat, F., Damotte, B., Mugnier, J.L., and Polino, R., 1996, The Ecors-Crop Alpine seismic traverse: *Bulletin de la Société Géologique de France*, v. 170, p. 1–113.
- Sacco, F., 1935, Note Illustrative della Carta Geologica d'Italia alla scala 1:100,000. Fogli di Torino, Vercelli, Mortara, Carmagnola, Asti, Alessandria, Cuneo, Ceva, Genova N. e Voghera O. costituenti il bacino terziario del Piemonte. Ministero delle Corporazioni, Regio Ufficio Geologico di Roma, 85 p.
- Sage, F., Collot, J.-Y., and Ranero, C.R., 2006, Interplate patchiness and subduction-erosion mechanisms: evidence from depth-migrated seismic images at the central Ecuador convergent margin: *Geology*, v. 34, n. 12, p. 997-1000.

- Saleeby, J., 1979, Kaweah serpentinite mélange, southwest Sierra Nevada foothills, California: Geological Society of America Bulletin, v. 90, p. 29-46.
- Saleeby, J., 2011, Geochemical mapping of the Kings-Kaweah ophiolite belt, California – Evidence for progressive mélange formation in a large offset transform-subduction initiation environment, *in* Wakabayashi, J., and Dilek, Y., eds., *Melanges: Processes of formation and societal significance*. Geological Society of America Special Paper 480, p. 31-73.
- Scholl, D. W., Vallier, T.L., and Stevenson A.J., 1987, Geologic evolution and petroleum geology of the Aleutian Ridge, *in* Scholl, D. W., Grantz, A., and Vedder, J. G., eds., *Geology and resource potential of the continental margin of western North America and adjacent ocean basins - Beaufort Sea to Baja California: Circum-Pacific Council for Energy and Mineral Resources, Earth Science Series*, v. 6, p. 124-155, Houston, Texas.
- Silver, E.A., and Beutner, E.C., 1980, *Melanges: Geology*: v. 8, p. 32–34.
- Singlenton, J.S., and Cloos, M., 2013, Kinematic analysis of mélange fabrics in the Franciscan Complex near San Simeon, California: Evidence for sinistral slip on the Nacimiento fault zone?: *Lithosphere*, v. 5, p. 179-188.
- Stampfi, G.M., and Borel, G.D., 2002, A plate tectonic model for the Paleozoic and Mesozoic constrained by dynamic plate boundaries and restored synthetic oceanic isochrones: *Earth and Planetary Science Letters*, v. 196, p. 17 - 33.
- Stampfi, G.M., Borel, G.D., Marchant, R., and Mosar, J., 2002, Western Alps geological constraints on western Tethyan reconstructions, *in* Rosenbaum, G., and Lister, G.S., eds., *Reconstruction of the evolution of the Alpine-Himalayan Orogen: Journal of the Virtual Explorer*, v. 7, p. 75 - 104.
- Strasser, M., Moore, G.F., Kimura, G., Kitamura, Y., Kopf, A.J., Lallemand, S., Park, J-O., Sreaton, E.J., Su, X., Underwood, M.B., and Zhao, X., 2009, Origin and evolution of a splay fault in the Nankai accretionary check: *Nature Geosciences*, v. 2, p. 648–652, doi:10.1038/ngeo609.
- Strasser, M., Moore, G.F., Kimura, G., Kopf, A.J., Underwood, M.B., Guo, J., and Sreaton, E.J., 2011, Slumping and mass transport deposition in the Nankai fore arc: Evidence from IODP drilling and 3-D reflection seismic data: *Geochemistry Geophysics Geosystems*, v.12, Q0AD13, doi:10.1029/2010GC003431.
- Taira, A., Hill, I., Firth, J., Berner, U., Bruckmann, W., Byrne, T., Chabernaud, T., Fisher, A., Foucher, J-P., Gamo, T., Gieskes, J., Hyndman, R., Karig, D., Kastner, M., Kato, Y., Lallemand, S., Lu, R., Maltman, A., Moore, G., Moran, K., Olafsson, G., Owens, W., Pickering, K., Siena, F., Taylor, E., Underwood, M., Wilkinson, C., Yamano, M., Zhang, J., 1992, Sediment deformation and hydrogeology of the Nankai trough accretionary prism: synthesis of shipboard results of ODP Leg 131: *Earth and Planetary Science Letters*, v. 109, p.431–450.
- Ukar, E., 2012, Tectonic significance of low-temperature blueschist blocks in the Franciscan mélange at San Simeon, California: *Tectonophysics*, v. 568-569, p. 154–169.
- Vai, G.B., and Castellarin, A., 1993, Correlazione sinottica delle unità stratigrafiche nell'Appennino Settentrionale, *in* Capozzi, R., and Castellarin, A., eds., *Studi preliminari all'acquisizione dati del profilo CROP 1-1a La Spezia-Alpi orientali: Studi Geologici Camerti, Volume Speciale 2*, p. 171-185.

- Vannucchi, P., and Bettelli, G., 2002, Mechanism of subduction accretion as implied from the broken formations in the Apennines, Italy: *Geology*, v. 30, n. 9, p. 835-838.
- Vannucchi, P., and Bettelli, G., 2010, Myths and recent progress regarding the Argille Scagliose, Northern Apennines, Italy, *in* Dilek, Y., ed., *Alpine Concept in Geology: International Geology Review*, v. 52, nos. 10–12, p. 1106–1137.
- Vannucchi, P., and Maltman, A., 2000, Insight into shallow-level processes of mountain building from the Northern Apennines, Italy: *Journal of Geological Society, London*, v. 157, p. 105–120.
- Vannucchi, P., Maltman, A., Bettelli, G., and Clennel, B., 2003, On the nature of scaly fabric and scaly clay: *Journal of Structural Geology*, v. 25, p. 673-688.
- Vezzani L., Festa, A., and Ghisetti, F., 2010, Geology and Tectonic evolution of the Central-Southern Apennines, Italy: *Geological Society of America Special Paper 469*, 58 p., accompanying by a CD-ROM including the “Geological-Structural Map of the Central-Southern Apennines (Italy)” at 1:250,000 scale, Sheets 1 and 2. doi: 10.1130/2010.2469.
- Vignaroli, G.L., Faccenna, C., Jolivet, L., Piromallo, C., and Rossetti, F., 2008, Subduction polarity reversal at the junction between the Western Alps and the Northern Apennines, Italy: *Tectonophysics*, v. 450, p. 34-50.
- von Huene, R., and Lallemand, S., 1990, Tectonic erosion along the Japan and Peru convergent margins: *Geological Society of America Bulletin*, v. 102, p. 704-720.
- von Huene, R., Ranero, C.R., Weinrebe, W., and Hinz, K., 2000, Quaternary convergent margin tectonics of Costa Rica, segmentation of the Cocos Plate, and Central American volcanism: *Tectonics*, v. 19, p. 314–334, doi:10.1029/1999TC001143.
- Wakabayashi, J., 2011, Mélanges of the Franciscan Complex, California: Diverse structural settings, evidence for sedimentary mixing, and their connection to subduction processes. *Geological Society of America Special Papers 480*, 117-141. doi: 10.1130/2011.2480(05).
- Wakabayashi, J., 2012, Subducted sedimentary serpentinite mélanges: Record of multiple burial–exhumation cycles and subduction erosion: *Tectonophysics*. V. 568-569, p. 230-274.
- Wakita, K., 2012, Mappable features of mélanges derived from Ocean Plate Stratigraphy in the Jurassic accretionary complexes of Mino and Chichibu terranes in Southwest Japan: *Tectonophysics*, v. 568-569, p. 74-85.
- Wang, K., and Hu, Y., 2006, Accretionary prisms in subduction earthquake cycles: The theory of dynamic Coulomb wedge: *Journal of Geophysical Research*, v. 111, B6, p. B06410, doi: 10.1029/2005JB004094.
- Yamamoto, Y., 2006, Systematic variation of shear-induced physical properties and fabrics in the Miura-Boso accretionary prism: the earliest processes during off-scraping: *Earth and Planetary Science Letters*, v. 244, p. 270-284.
- Yamamoto, Y., Nidaira, M., Ohta, Y., and Ogawa, Y., 2009, Formation of chaotic rock units during primary accretion processes: examples from the Miura-Boso accretionary complex, central Japan: *Island Arc*, v. 18, p. 496-512.

1153  
1154 Yamamoto, Y., Yamada, Y., Yamashita, Y., Chiyonobu, S., Shibata, T., Hojo, M., 2012, Systematic  
1155 development of submarine slope failures at subduction margins: fossil record of accretion-related  
1156 slope failure in the Miocene Hota Accretionary Complex, Central Japan, *in* Yamada, Y.,  
1157 Kawamura, K., Ikehara, K., Ogawa, Y., Urgeles, R., Mosher, D., Chaytor, J., and Strasser, M.,  
1158 eds., Submarine mass movements and their consequences. *Advances in Natural and*  
1159 *Technological Hazards Research* 31, p. 355-364.  
1160

1161



## Figure captions

**Figure 1** – (A) Structural sketch map of the northwestern Italy (modified from Bigi et al., 1983; Marroni et al., 2010; Mosca et al., 2010; Vezzani et al., 2010). (B) Location of Figure 1A. (C) Geological cross section across the northern sector of the *Tertiary Piedmont Basin* and Po plain (modified from Bello and Fantoni, 2002). The trace of the section is shown in Figure 1A. (D) Schematic crustal-scale cross section across the Western Alps to the *Tertiary Piedmont Basin* (modified from Roure et al., 1996; Stampfli et al., 2002). The section line is shown in Figure 1A.

**Figure 2** –Paleogeographic reconstruction (in map and in section) of the western Tethyan realm in (A, B) the Late Cretaceous (modified after Stampfli and Borel, 2002 and Stampfli et al., 2002 for map view; Vignaroli et al., 2008 and Marroni et al., 2010 for section view) and (C-D) middle-late Eocene times (modified after Castellarin, 1994; Festa et al., 2010b; Mosca et al., 2010 for map view; Marroni et al., 2010, for section view).

**Figure 3** – Stratigraphic columns of the External Ligurian Units in the Northern Apennines and Monferrato, and of the overlying Epiligurian and *Tertiary Piedmont Basin* successions. Modified from Marroni and Pandolfi (2007); Marroni et al. (2001, 2010); Codegone et al. (2012b).

**Figure 4** – (A) Simplified geological-structural map of the study area (location in Fig. 1A), showing the structural relationships between different chaotic rock units. (B) Geological cross section.

**Figure 5** – *Broken Formation*: (A) Schematic 3D drawing of an outcrop exposure (North of Gerbole) showing the different degrees of layer-parallel extension in two orthogonal directions. Asymmetrical boudinage, pinch-and-swell features, and R and R' shears characterize the WNW-striking section; symmetrical flattening and boudinage are present on the NNE-striking section. (B) Schematic 3D

drawing of an outcrop exposure (North of Gerbole), showing (a) the geometry of intralayer folds that show a sheath-like geometry on the NNE-stringing section. Note the asymmetric boudinage of fold limbs on the WSW-striking section. (b) 3D model of the intralayer fold showing the curvilinear fold axis. (C) Line-drawing of a polished hand sample, showing the asymmetric boudinage associated with extensional shearing and *in situ* disruption of alternating layers of sandstone (black) and shale (white) (NW of Gerbole). Black lines indicate R-shears. (D) Photograph showing a close-up of Fig. 5C. Black lines indicate R-shears. (E) Photograph of a polished surface of hand sample showing C'-type shears (*sensu* Passchier and Trouw, 2002; see white lines) that transecting the varicolored shaly layers (North of Piazzo). (G) SEM image showing anastomosing domains of flattened clay particles, transected by C'-type shears (*sensu* Passchier and Trouw, 2002; see white lines).

**Figure 6** –Diagrams showing different organizational types of the blocks and the rock fabric in diverse types of chaotic rock units: (A) Aspect ratio (blocks long axis/short axis) versus block long axis. (B) Aspect ratio (blocks long axis/short axis) versus location of chaotic units (i.e., distance from the thrust faults). Data are plotted as means with 95% error bars indicated. (C) Mesoscale data (Schmidt net, lower hemisphere) of scaly fabric, lineation of the long-axis of the blocks, and folds of *Broken Formation*, *Tectonic Mélange* and *Diapiric Mélange*.

**Figure 7** – *Tectonic Mélange*: (A) Line-drawing of an outcrop exposure (SW of la Pietra), showing the “structurally ordered” block-in-matrix fabric related to a NE-verging reverse shear (black lines). Dark-gray color indicates both native and exotic blocks (see text); white color indicates the shaly matrix. (B) Close-up of Fig. 7A. The photograph shows elongated to phacoidal blocks embedded in the scaly matrix that is pervasively affected by an S-C fabric. (C) Line-drawing of polished hand sample, showing the reorientation of elongated blocks (dark-gray color) to S-C fabric (black lines). White color indicates the shaly matrix (NW of Gerbole). (D) SEM image of the shaly matrix, showing the S-C fabric (white dashed lines). The arrow indicates an elongated clast aligned parallel to the C-shear surface.

1214

1215 **Figure 8 – *Diapiric Mélange*:** (A) Detailed geological map of the diapiric body located to the NE of  
 1216 Piazzo (location in Fig. 4A). Note the irregular rounded shape and the two-fold zonation of  
 1217 deformation, which is characterized by marginal and core zones (see text for major details). The  
 1218 intrusive contact (white dashed line) crosscuts the NW-striking bedding of the Broken formation and  
 1219 the structural fabric of the *Tectonic Mélange*. (B) Core zone: tabular and phacoidal limestone and  
 1220 sandstone blocks aligned parallel to the sub-vertical fluidal fabric of the shaly matrix (NE of Piazzo).  
 1221 (C) Close-up of the marginal zone: elongated calcareous marly block aligned parallel to the sub-  
 1222 vertical flow fabric of the varicolored shaly matrix (NE of Piazzo). (D) Close-up of the transition zone  
 1223 between the *Diapiric* and *Sedimentary Mélanges*: the polished surface of a hand sample in top-view  
 1224 showing the inclusion of part of the *Diapiric Mélange* (central part of the photograph) in a brecciated  
 1225 matrix, which was developed during the emplacement of the Sedimentary Mélange (NE of Pareglia).  
 1226 (E) SEM image of the matrix in the core zone showing irregular and convolute folds (marked by  
 1227 dashed white lines) affecting the clay particle alignment. Clay surfaces gently wrap around elongated  
 1228 and lenticular clasts (white arrows). (F) SEM image of the matrix in the marginal zone, showing the  
 1229 finely-spaced alignment of clay particles that define sigmoid-shaped sub-vertical domains. White  
 1230 arrows indicate shear surfaces.

1231

1232 **Figure 9 – *Sedimentary Mélange*** (i.e., Polygenetic argillaceous breccias): (A) Highly disordered block-  
 1233 in-matrix fabric. Variably-shaped blocks (equidimensional, tabular, phacoidal and irregular) of  
 1234 limestone, sandstone, marl and siltstone randomly float in the brecciated shaly matrix (NW of  
 1235 Gerbole). (B) Polished surface of hand sample showing the isotropic texture of the brecciated shaly  
 1236 matrix of Fig. 9A. (C) Polished surface of hand sample, showing the superposition along an erosive  
 1237 surface (white arrows) of a brecciated lenticular body onto extensionally sheared, varicolored shaly  
 1238 layers (North of Piazzo). (D) SEM image of the brecciated matrix of the hand sample of Fig. 9B.  
 1239 Rounded and irregular-shaped clasts (dashed white lines) randomly float in a clayey matrix (dashed

black lines). (F) SEM image of the brecciated matrix of the hand sample of Fig. 9C. The arrow indicates the gradual decrease of the spacing between clay particles from the clast-supported to clast-poor part of the rocks.

**Figure 10 – Sedimentary Mélange** (i.e., Polygenetic argillaceous breccias): (A) Simplified structural map, showing the structural relationships between different chaotic rock units and the direction of emplacement of *Sedimentary Mélange* bodies (i.e., Polygenetic argillaceous breccias). Rose diagrams show the sub-radial distribution of the direction of extensional shearing measured at the base of the Polygenetic argillaceous breccias. (B) Polished surface of hand sample of the basal part of the *Sedimentary Mélange*. Extensionally sheared layers show a planar anisotropy crosscut by low-angle extensional shear surface (R-shear) (North of Piazze). (C) SEM image of the matrix in Fig. 10B, showing the alignment of elongated clasts and compacted clay particles truncated by C'-type shears (*sensu* Passchier and Trouw, 2002; see white arrows).

**Figure 11 – Shale dike injections:** (A) Line-drawing of an outcrop exposure, showing shale dike injections (grey color) intruding into the brecciated matrix of the Polygenetic argillaceous breccias (white color). Elongated blocks (black color) are reoriented by the sub-vertical shale injections (NE of Piazze). (B) Close-up of Fig. 11A. Dashed white lines mark the margins of the blocks and of the shale dike injections. (C) Close-up of Fig. 11A. Tabular block aligned parallel to the sub-vertical fluidal features of the shale dike injection. (D) Polished surface of hand sample showing a subvertical flame-shaped injection of red shale within the brecciated matrix of the Polygenetic argillaceous breccias. Elongated limestone and sandstone clasts are rotated and aligned parallel to the intrusive contacts (NE of Pareglia). (E) SEM image of the matrix of a shale dike injection showing irregular to isoclinal folds (white lines) affecting the flow fabric of the finely spaced clay particles. White arrows indicate rounded clasts. (F) SEM image showing a close-up of an irregular fold.

**Figure 12** – (A) Conceptual model for the evolution of the Ligurian accretionary wedge during the Late Cretaceous – middle Eocene (accretionary stage). Not-to-scale. (B) Block diagram showing the deformation of sediments prior to accretion. Vertical compaction of unconsolidated sediments occurs prior to accretion, forming a symmetrical boudinage. The increasing shear during the approach to the toe of the accretionary wedge promotes asymmetrical boudinage and development of R-shears in more competent layers. (C) Block diagram showing the deformation of sediments within the toe of the accretionary wedge. Heterogeneous deformation results in the contemporaneous production of flattened, intralayer, sheath like folds, layer-parallel extensional fabric, and asymmetric boudinage. This heterogeneous deformation is likely related to the inclination of sedimentary layers with respect to the  $\sigma_1$  (see Kusky and Bradley, 1999). See text for a detailed discussion.

**Figure 13** –Conceptual model for the evolution of the Ligurian accretionary wedge during late Oligocene intracollisional deformation. The superposition of tectonic, diapiric and sedimentary processes occurred in this short time span. (A) Thrusting related to NE-verging regional shearing formed the *Tectonic Mélange*. This is characterized by (A') a structurally ordered block-in-matrix fabric produced by mixing of the exotic and native blocks that are wrenched from the overlying units (see stratigraphic column in Fig. 13A). (B) *Diapiric Mélange* formed by the upward rise of unconsolidated sediments that are triggered by overpressurized fluids, which are concentrated along the shear surface of thrust faults. (C) *Sedimentary Mélange* (i.e., Polygenetic argillaceous breccias) formed by the collapse of the margins of the topographic high formed by the emergence of a diapiric body on the seafloor. (C') Downslope emplacement of *Sedimentary Mélanges* units sealed the thrust faults, superposing the External Ligurian Units on the late Eocene–Oligocene Tertiary Piedmont Basin sedimentary succession. Shale dike injection is triggered by the combined effect of sedimentary loading (provided by the emplacement of the *Sedimentary Mélange*) and discharge of fluids after the thrust faulting stage, intrudes into the *Sedimentary Mélange* (i.e., Polygenetic argillaceous breccias). (C'') Close-up of a shale dike injections into the block-in-matrix fabric of the *Sedimentary Mélange*.

1292

1293 **Table 1** – Diagnostic structural features observed at the map-to meso- and micro-scales in the *Broken*  
1294 *Formation* and in the *Tectonic, Diapiric* and *Sedimentary Mélanges*.

Figure 1  
[Click here to download high resolution image](#)

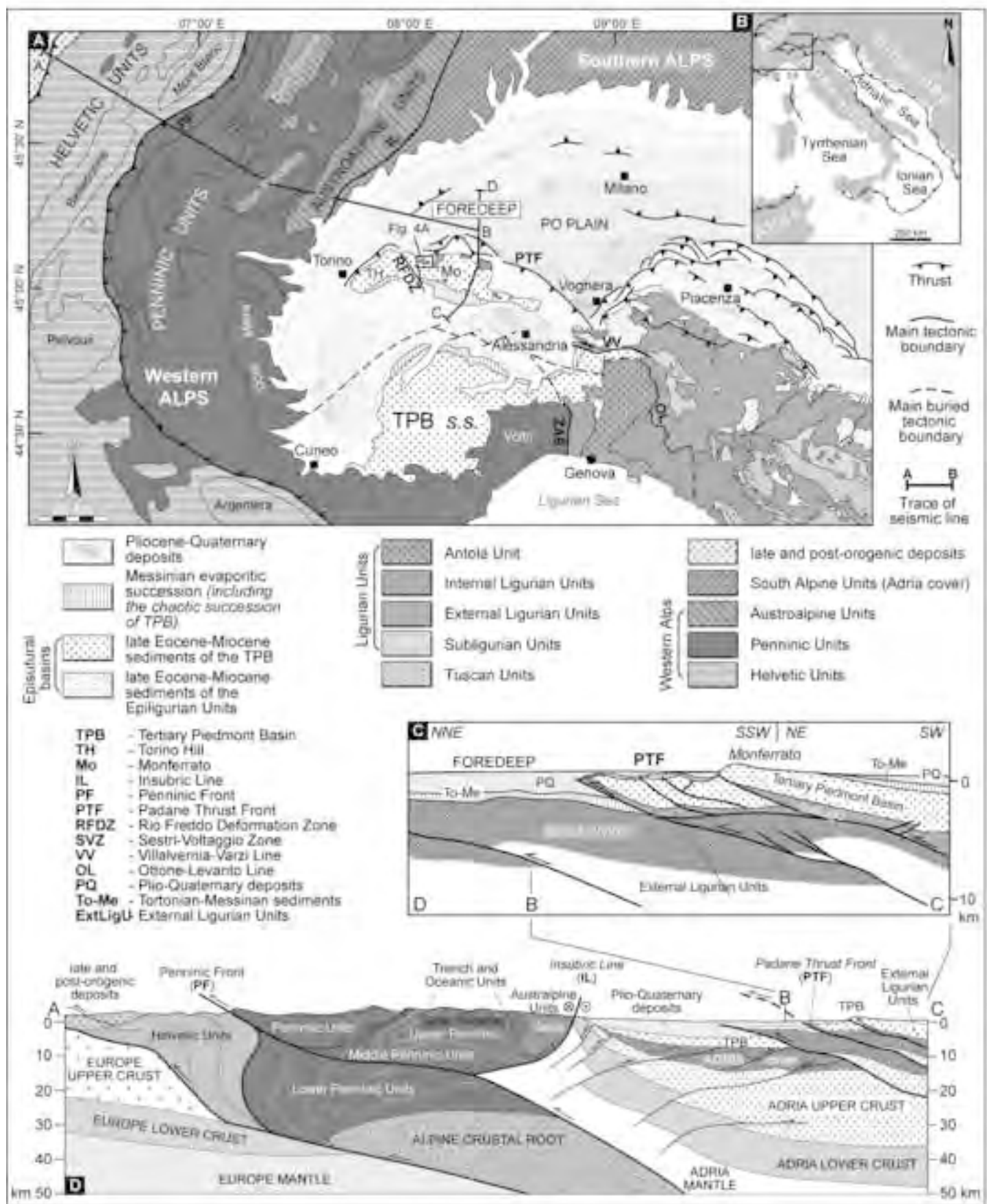


Figure 1 - Festa et al. (\*.jpg)

Figure 2

[Click here to download high resolution image](#)

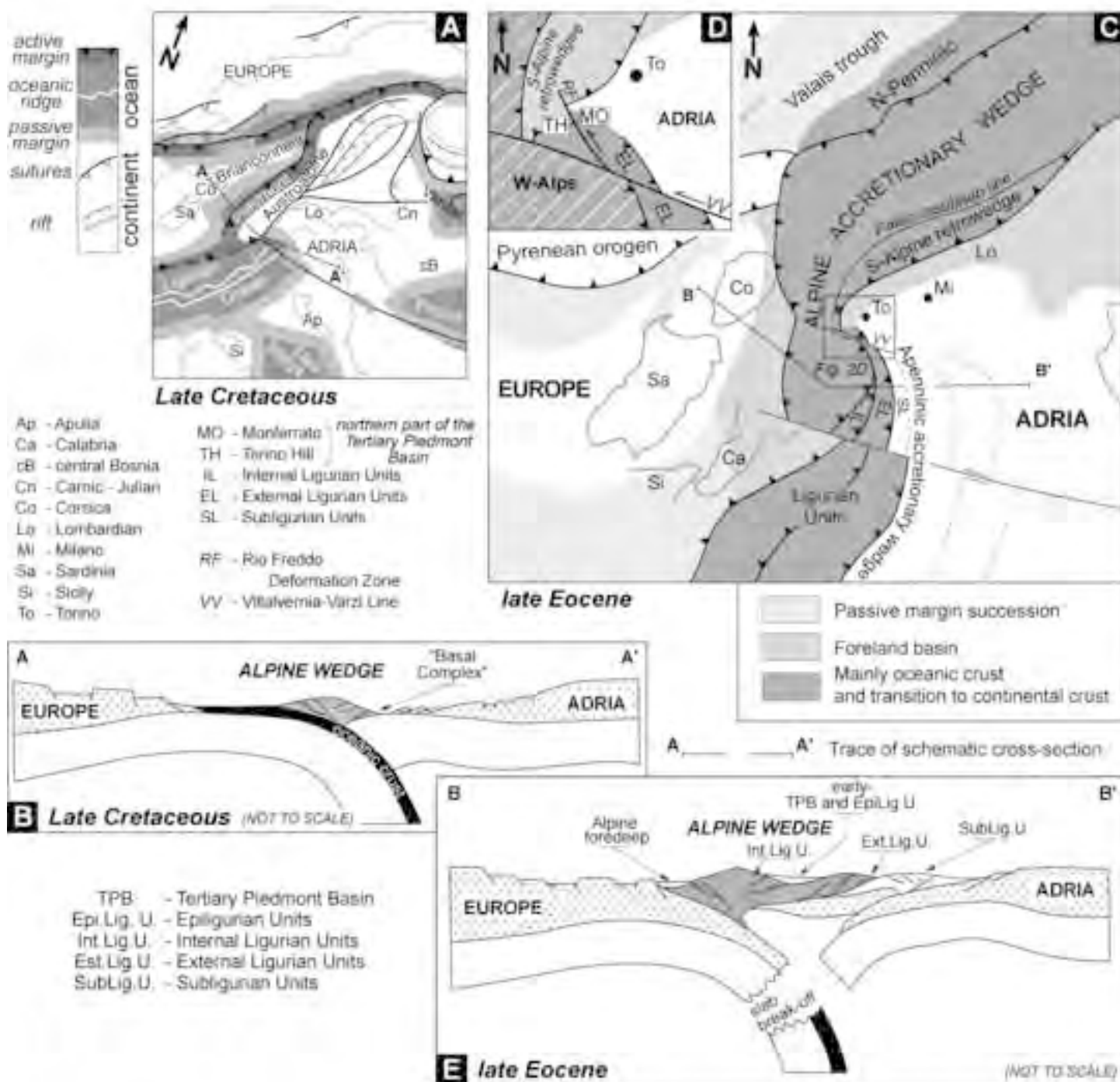


Figure 2 - Festa et al. (\*.jpg)





Figure 4 (Revised)

[Click here to download high resolution image](#)

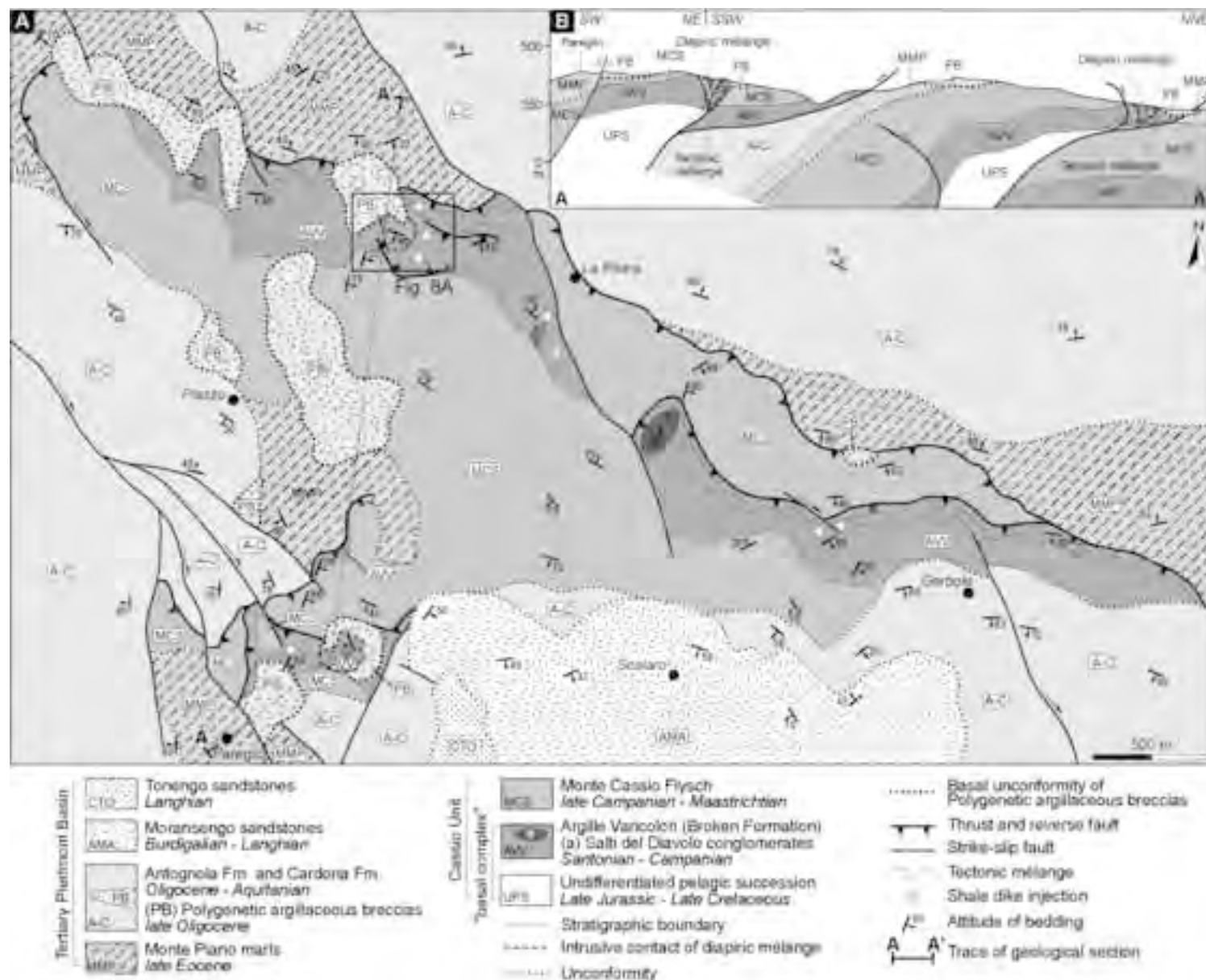


Figure 4 - Festa et al. (\*.jpg)

Figure 5  
[Click here to download high resolution image](#)

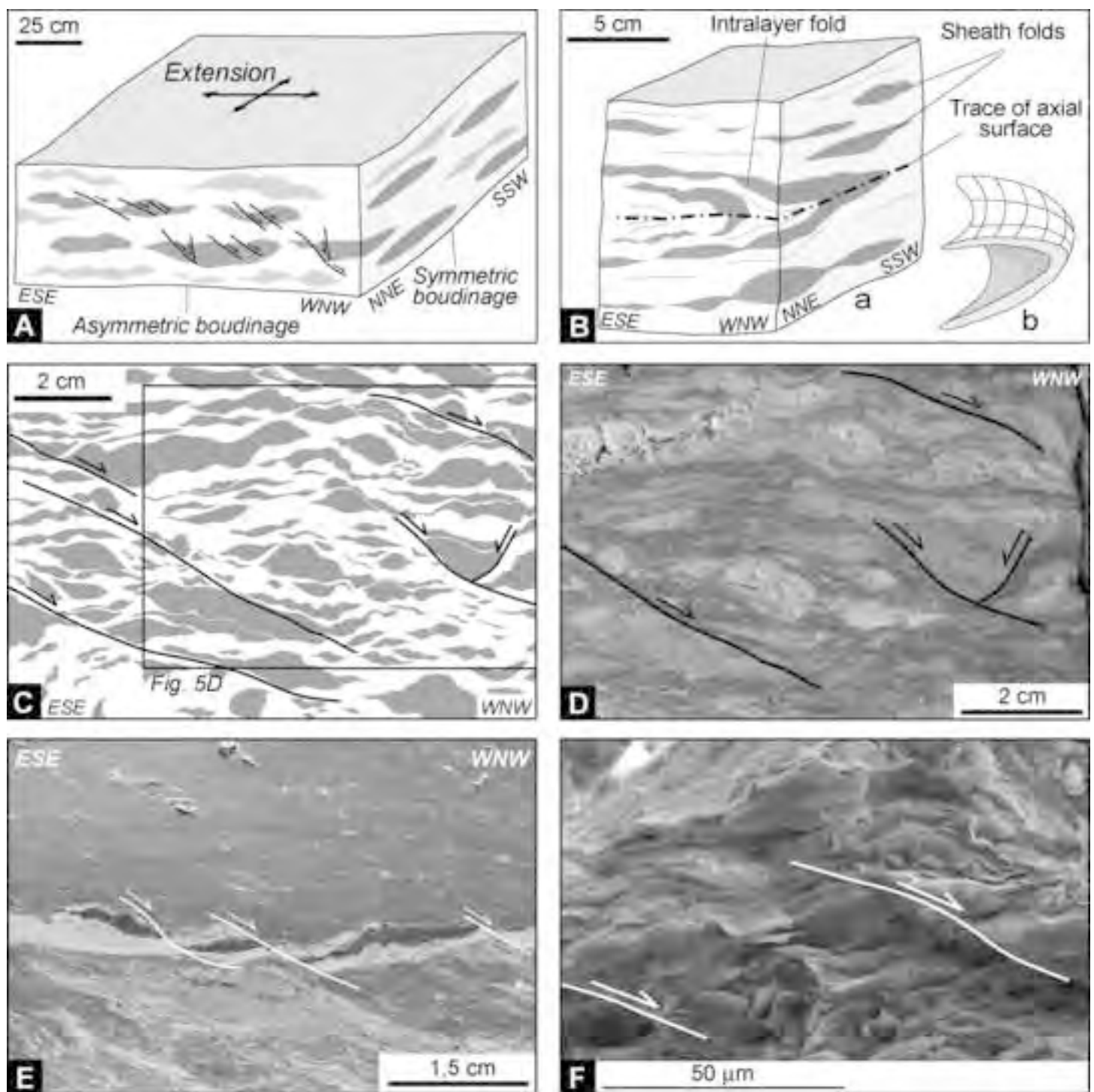


Figure 5 - Festa et al. (\*.jpg)



Figure 6  
[Click here to download high resolution image](#)

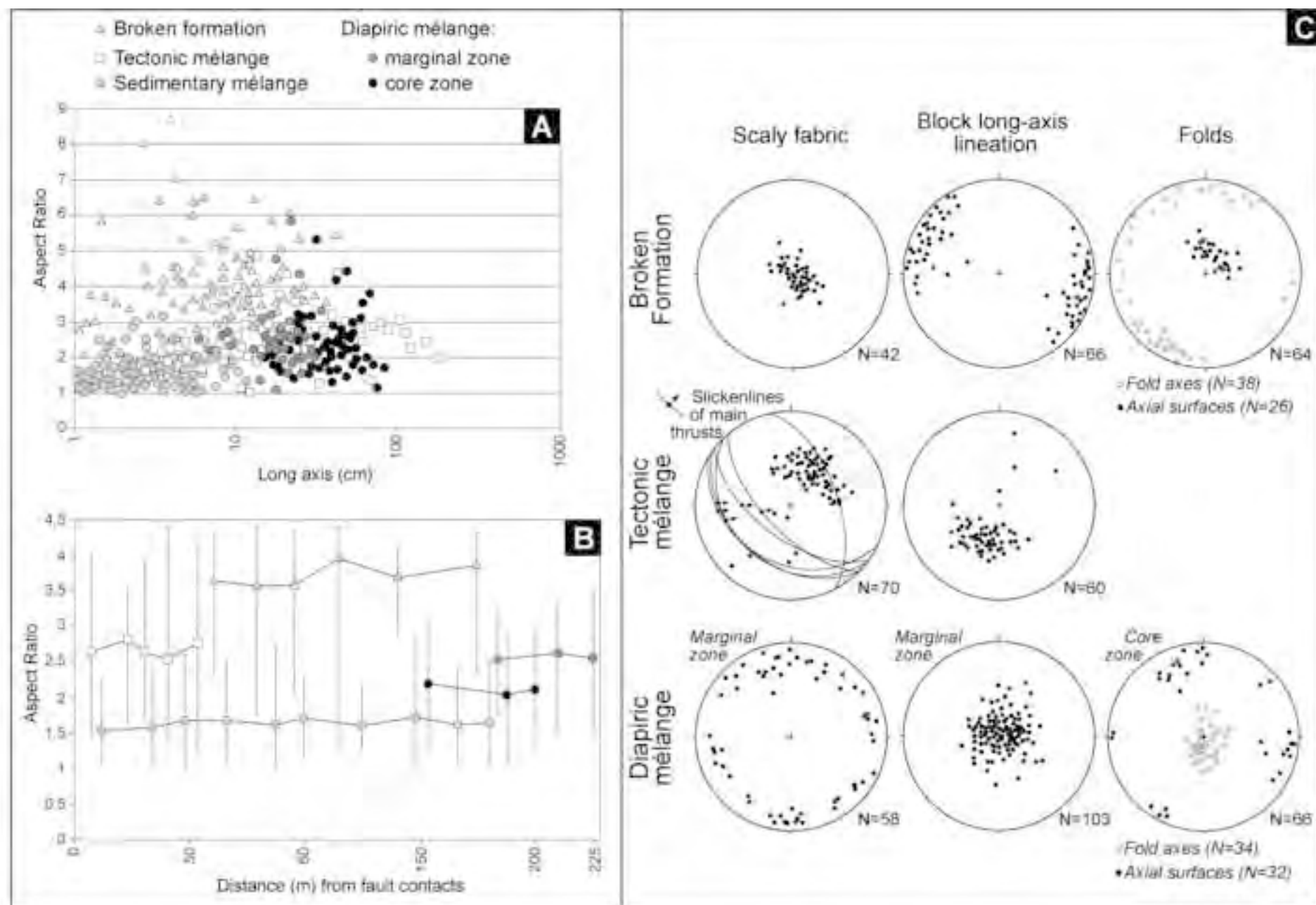


Figure 6 - Festa et al. (\*.jpg)

Figure 7  
[Click here to download high resolution image](#)

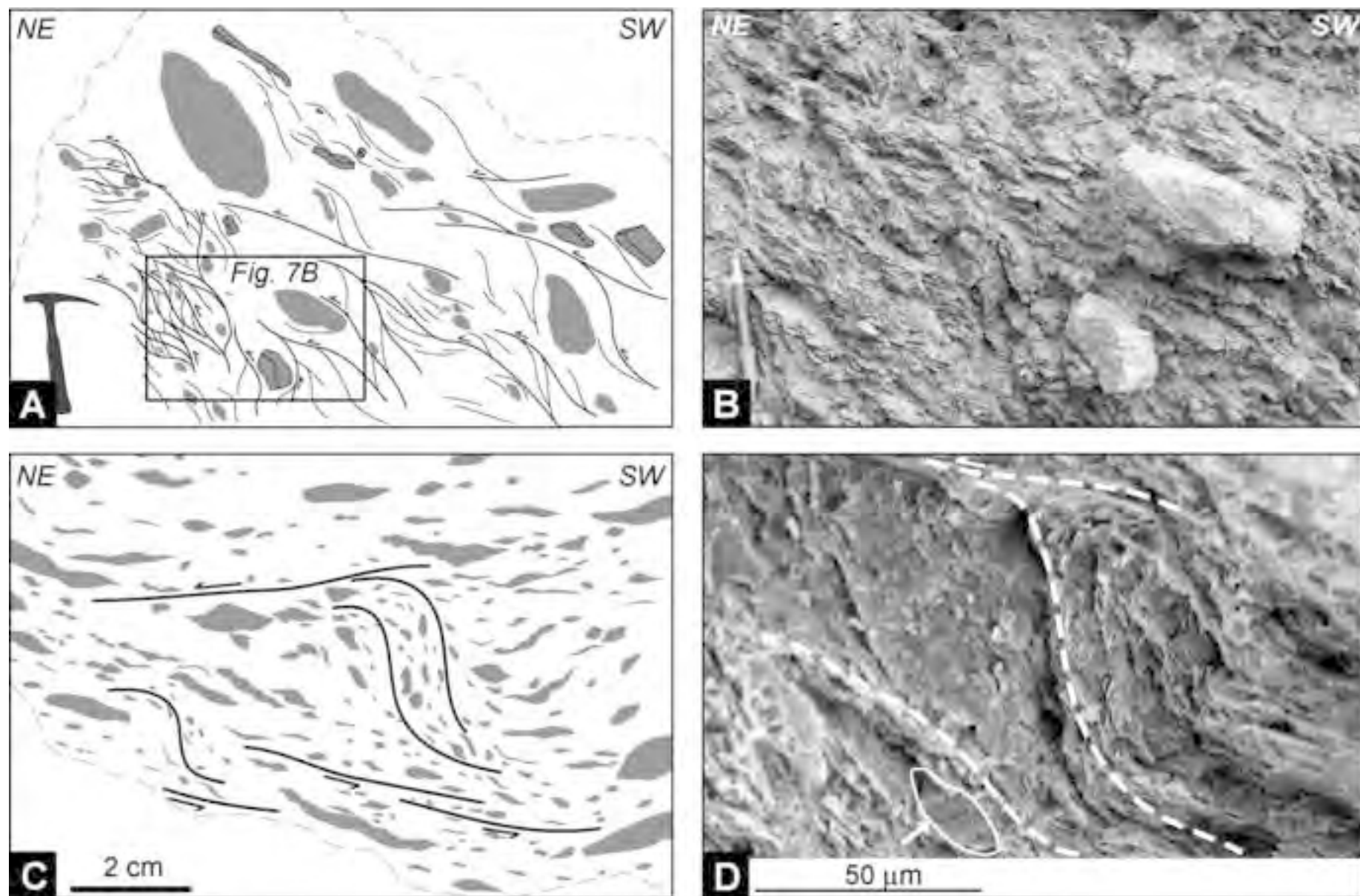


Figure 7 - Festa et al. (\*.jpg)

Figure 8  
[Click here to download high resolution image](#)

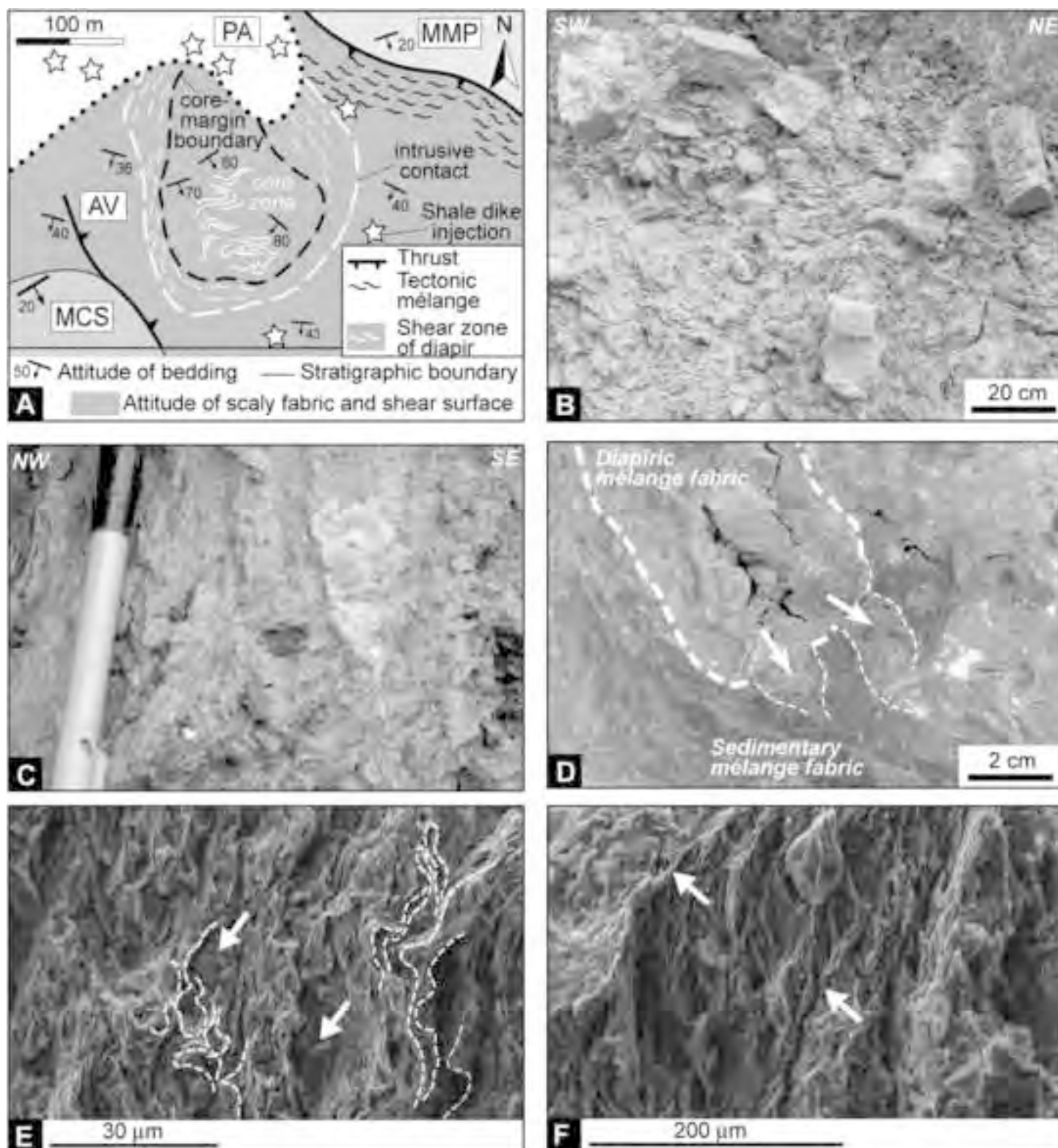


Figure 8 - Festa et al. (\*.jpg)



Figure 9  
[Click here to download high resolution image](#)

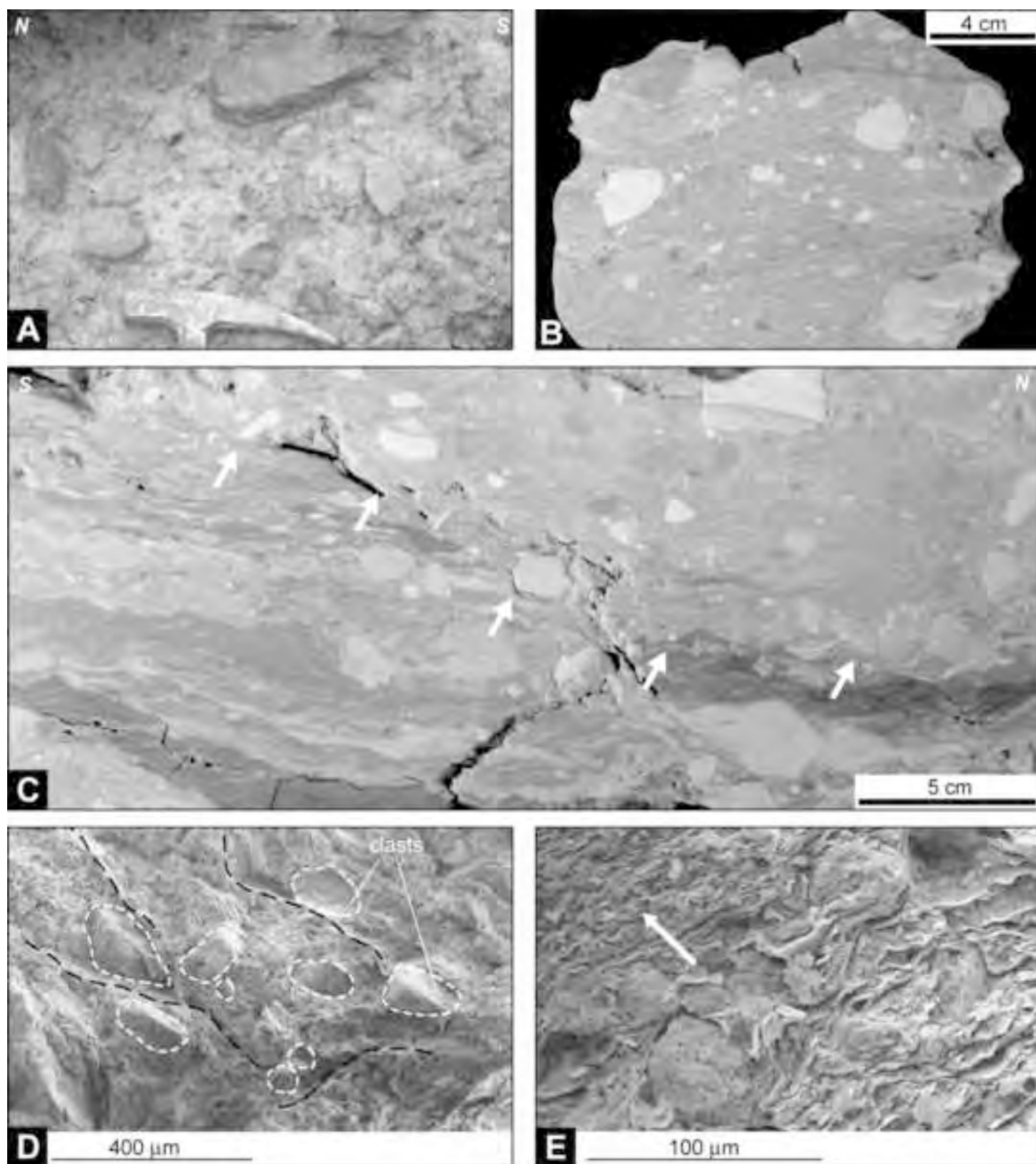


Figure 9 - Festa et al. (\*.jpg)

Figure 10  
[Click here to download high resolution image](#)

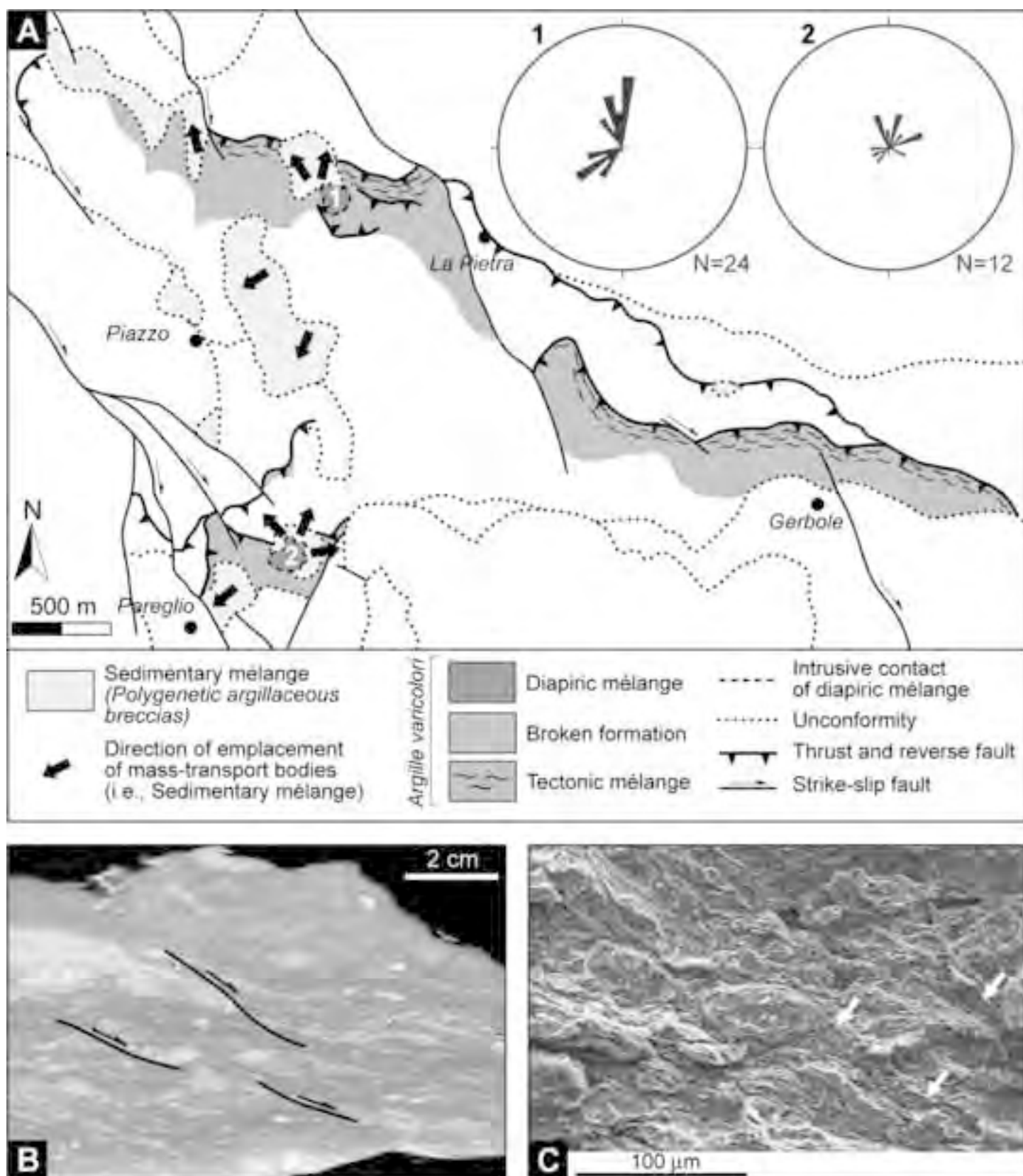


Figure 10 - Festa et al. (\*.jpg)



Figure 11  
[Click here to download high resolution image](#)

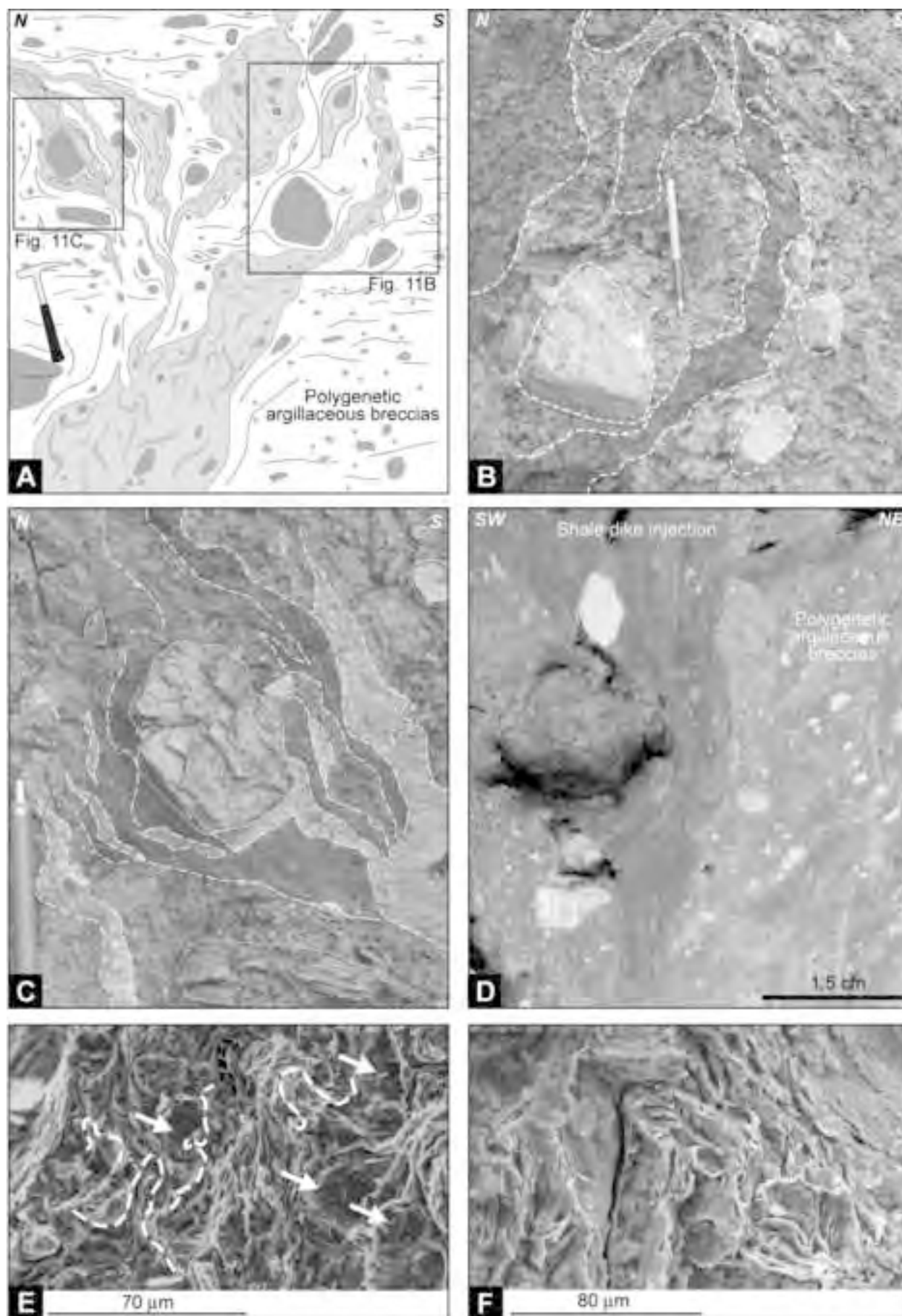


Figure 11 - Festa et al. (\*.jpg)

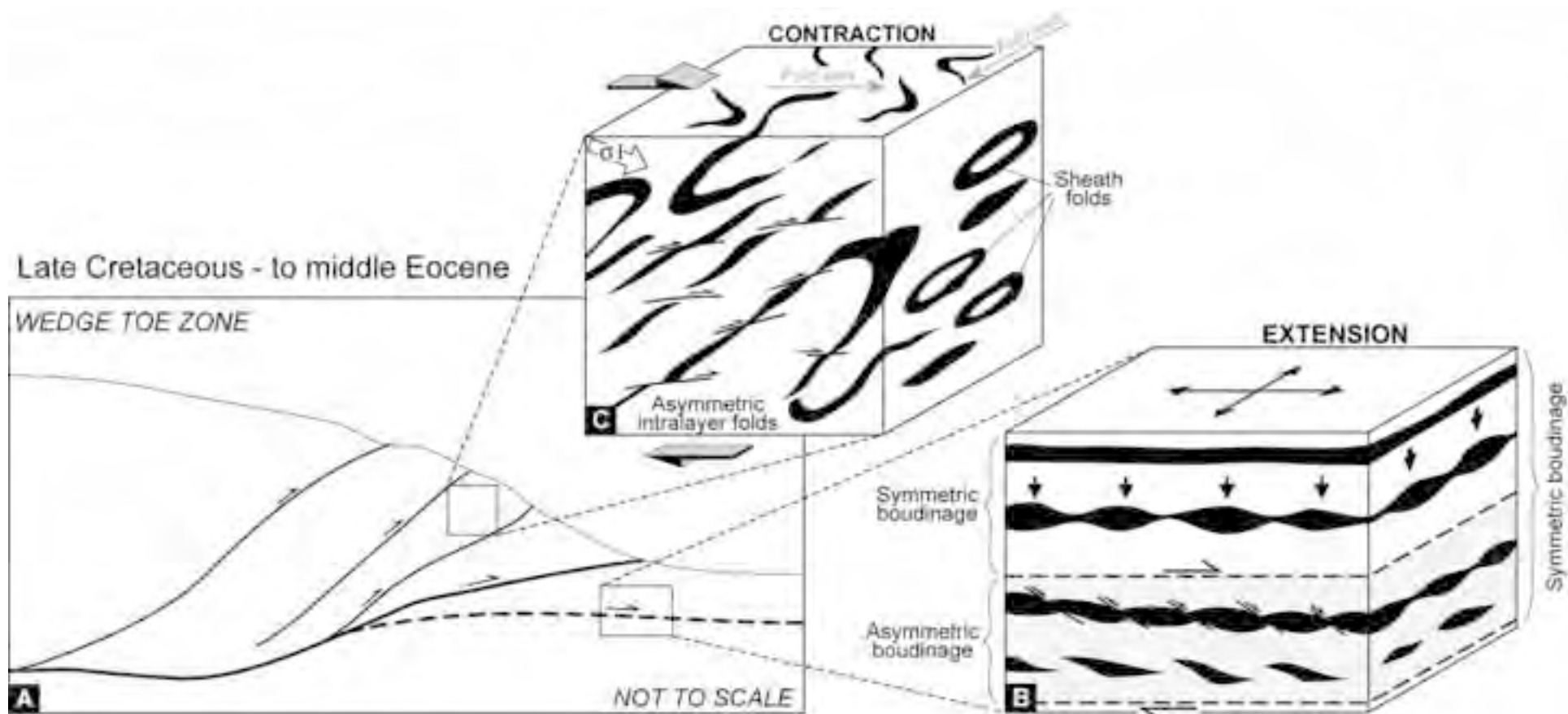


Figure 12 - Festa et al. (\*.jpg)

[Click here to download high resolution image](#)

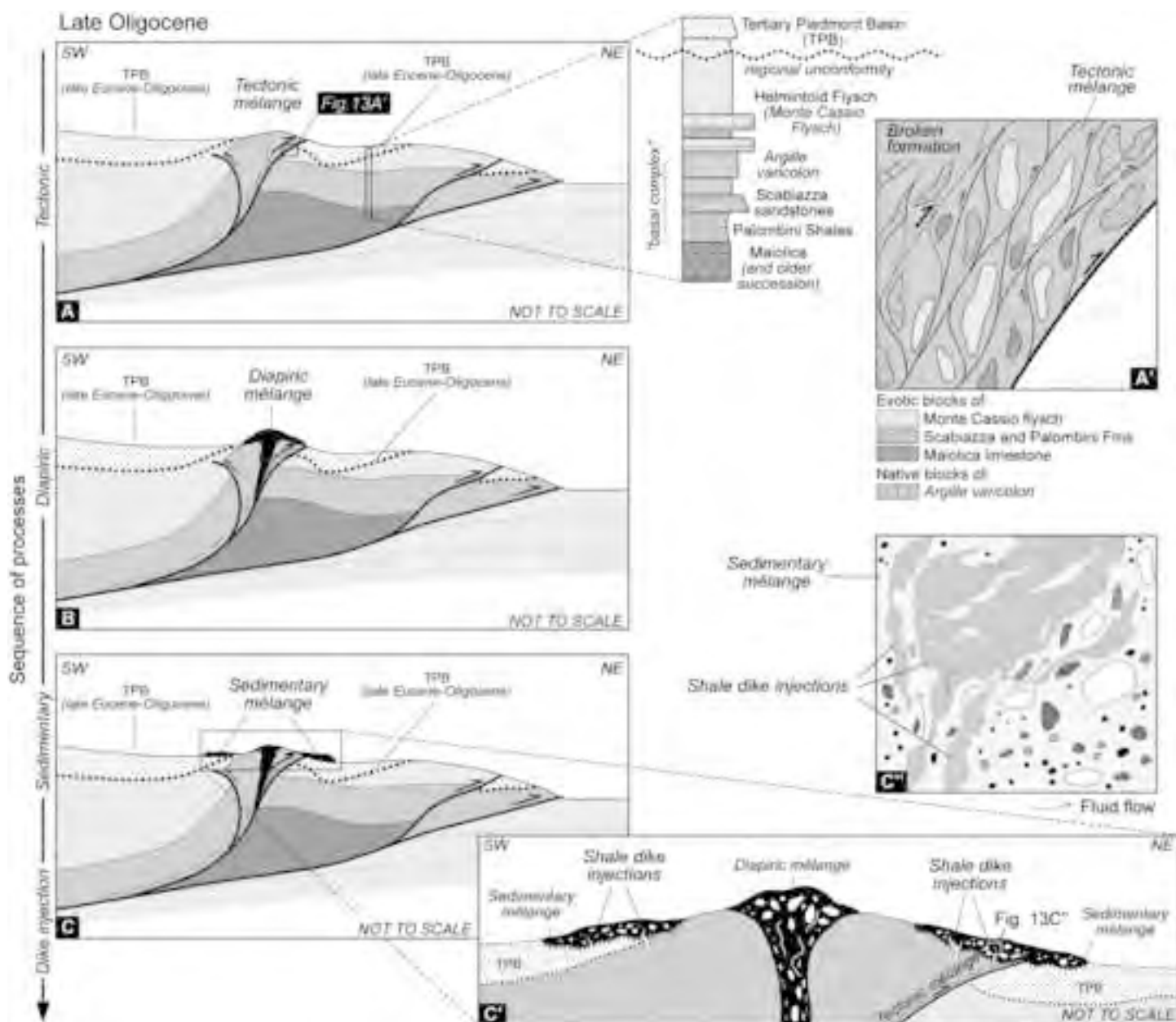


Figure 13 - Festa et al. (\*.jpg)

TABLE 1.

		Broken Formation	Tectonic M $\acute{e}$ lange	Diapiric M $\acute{e}$ lange	Sedimentary M $\acute{e}$ lange
Process of formation		Tectonic		Diapiric	Sedimentary (gravitational)
Map-scale features	Shape of chaotic unit (in map view)	Aligned to conformable stratigraphic contacts of bounding lithostratigraphic units	Narrow and elongated; aligned to thrusts	Circular to elliptical	Irregular
	Nature of bounding surface	No bounding surface: gradual transition to both Tectonic M $\acute{e}$ lange and coherent lithostratigraphic units	Fault (i.e., thrust)	High angle intrusive contacts	Lower and upper depositional contacts as discontinuity surfaces
Meso-scale features	Block-in-matrix fabric	Progressive distribution from continuous layering to boudinage up to isolated blocks aligned to the original coherent bending (i.e., pseudo-bedding) Non-cylindrical, flattened intralayer folds with curvilinear axial surfaces	Structurally ordered fabric (S-C and/or P-T shears) consistent with the regional shortening direction	Zonation of deformation: - <u>Core zone</u> : plurimetric, irregular non-cylindrical folds with steeply dipping axes and irregular axial trends; - <u>Marginal zone</u> : pervasive vertical scaly fabric and fluidal features which wrap around the blocks	Random distribution of blocks in a brecciated isotropic matrix
	Nature of blocks	Native (i.e., intra-formational)	Native (i.e., intra-formational) and exotic (i.e., extra-formational)		
	Shape of blocks	From flat to ellipsoidal shape (aspect ratio: 3,5-4)	Phacoidal and tabular blocks (aspect ratio: 2,5-2,8)	- <u>Core zone</u> : irregular blocks (aspect ratio: 2,1-2,3) - <u>Marginal zone</u> : phacoidal blocks (aspect ratio: 2,5-2,6)	Angular to rounded and irregular blocs (aspect ratio: 1,5-1,7)
	Size of blocks	mean: 33 cm max: 50 cm	- Native blocks: mean: 33 cm; max: 50 cm - Exotic blocks: mean: 35 cm; max: 125 cm	- <u>Core zone</u> : mean: 60 cm; max: 90 cm - <u>Marginal zone</u> : mean: 25 cm; max: 40 cm Sub-vertical flow fabric.	mean: 4 cm max: 15 cm
	Matrix fabric	Anastomosing domains of clays aligned to bedding. Locally, the fabric is transected by C' and/or R shears	Clays rotated and aligned to S-C fabric which isolate sigmoidal to lenticular shaped micro-lithons. Occurrence of striation.	- <u>Core zone</u> : alignment of irregularly anastomosing and folded clays (sub-vertical axial fold); - <u>Marginal zone</u> : sub-vertical S-C fabric	Anastomosing domains of clays that, close to the basal erosional surface, are transected by C'-type shears
Micro-scale features	Clast arrangement	Planar orientation of elongated clasts, locally transected by R-shears	Alignment of elongated clasts to the S-C fabric	Alignment of elongated clasts to the fluidal fabric	Random distribution of equidimensional and irregular clasts. Close to the basal surface, elongated clasts are aligned to the clays

Table 1 – Festa et al. (\*.doc)